Proteomes
Proteoforms-to-Systems

MDPI

Review

Proximity Labeling Comes into Focus: Spatial Interactomics of the DNA Damage Response

Sisi Qin [1,†], Jeongmin An [2,3,†], Siyao Tang [4], Zhichao Xu [4], Gayoung Seo [2,3,*] and Wootae Kim [2,3,*]

1 Department of Pathology, University of Chicago, Chicago, IL 60637, USA; sisiq@uchicago.edu
2 Department of Integrated Biomedical Science, Soonchunhyang Institute of Medi-bio-Science (SIMS), Soonchunhyang University, Cheonan 31151, Republic of Korea; anjeongmin@sch.ac.kr
3 Institute for Molecular Metabolism Innovation, Soonchunhyang University, Asan 31538, Republic of Korea
4 College of Biology, Hunan University, Changsha 410082, China; 15116338820@163.com (S.T.); xuzhichao811@163.com (Z.X.)
* Correspondence: gayoungs@sch.ac.kr (G.S.); wootaek@sch.ac.kr (W.K.)
† These authors contributed equally to this work.

Abstract

The DNA damage response is a problem of space and time: repair factors assemble at discrete lesions within seconds, organize into foci and biomolecular condensates, and disperse once repair is complete. These interactions are weak, transient and substoichiometric, precisely what affinity purification–mass spectrometry recovers least reliably. Proximity labeling (PL), in which a bait-fused enzyme covalently tags its neighborhood in living cells, suits this problem: it records interactions in situ and survives the lysis needed to solubilize chromatin. PL has been surveyed as a technology but not synthesized around genome maintenance. We organize the field by biological problem rather than by enzyme: double-strand break repair foci and condensates, the replication fork under stress, structure-specific lesions including R-loops and DNA–protein crosslinks, locus-directed mapping, and large repair scaffolds. The most tractable open problems are the interior proteome of repair condensates, the immediate neighborhood of a DNA–protein crosslink, and a controlled comparison of fork rewiring across genotoxic stresses. We weigh equally what decides whether a nuclear PL dataset is trustworthy, namely labeling radius versus chromatin crowding, enzyme residue bias, the mismatch between labeling and damage-signaling kinetics, fusion artifacts, peroxidase-substrate genotoxicity, and the reporting of gene products rather than proteoforms.

Keywords: proximity labeling; BioID; TurboID; APEX2; DNA damage response; genome stability; spatial interactomics; biomolecular condensates; replication stress; DNA–protein crosslinks

Check for updates

Received: 13 October 2026
Revised: 15 November 2026
Accepted: 19 November 2026
Published: 23 November 2026

Copyright: © 2026 by the authors. Licensee MDPI, Basel, Switzerland. This article is an open access article distributed under the terms and conditions of the Creative Commons Attribution (CC BY) license.

1. Introduction

Genome maintenance depends on the ordered, rapid, and reversible assembly of protein complexes at sites of DNA damage. The histone mark γH2AX appears within a minute of a double-strand break (DSB) and spreads over megabases of flanking chromatin across the following tens of minutes [1,2]; MDC1 docks on it [3], the RNF8/RNF168 ubiquitin cascade fires [4], and 53BP1, which requires a nucleosome carrying both the new ubiquitin mark and a constitutive methylation mark [5], nucleates large chromatin domains that recruit downstream effectors, while BRCA1–BARD1 drives the opposing, resection-dependent arm of the response [6], which BARD1 confines to post-replicative chromatin by reading unmethylated H4K20 [7]. These domains persist for hours, but the order in which

effectors arrive and the exchange of molecules within them play out over seconds to minutes; the resulting competition between end protection and end resection is what sets repair pathway choice [8,9], and the surrounding chromatin must be remodeled for each of these steps to proceed [10]. Replication forks recruit and shed accessory factors continuously as they encounter obstacles. R-loops, DNA–protein crosslinks (DPCs), and other bulky lesions each assemble a distinct local proteome. These interactions are transient, substoichiometric, spatially restricted, and often driven by post-translational modification (PTM) rather than by stable stoichiometric binding, with the damage-induced phosphoproteome alone running to hundreds of sites on repair factors [11]. Those same features are what make them difficult to capture by conventional biochemistry. Recent work makes the point concretely: long-range end resection is released in distinct phases by a DSB-bound proteasome variant acting through ubiquitin removal and targeted degradation in spatially separated compartments, a regulatory logic that no bulk, stability-based purification would resolve [12].

Affinity purification–mass spectrometry (AP-MS) remains the workhorse of interaction proteomics, but it recovers an interaction only if the complex survives cell lysis and washing intact. Weak or fast-exchanging partners dissociate; chromatin-bound baits require harsh extraction that further destabilizes complexes; and a factor that spends only seconds at a lesion is unlikely to be co-purified in proportion to its functional importance. Proximity labeling (PL) circumvents these limitations by moving the interaction-recording step inside the living cell. An engineered enzyme fused to a bait protein generates a short-lived reactive species that covalently biotinylates proteins within a defined radius; because the tag is a covalent modification, subsequent lysis can be as harsh as necessary, and the labeled neighborhood is recovered by streptavidin affinity purification and identified by mass spectrometry [13]. The conceptual ancestor of this strategy, DamID, tethered a DNA adenine methyltransferase to a chromatin protein to mark nearby genomic DNA [14]; contemporary PL applies the same logic of enzyme-tethered proximity marking to the proteome.

Proximity labeling has been reviewed extensively as a technology, and its application to the nucleus and to chromatin has been surveyed in general terms [15], most recently in a 2026 account of the chemical toolbox available for chromatin interactomics [16]. It has also appeared as one method among several in broader catalogs of DDR proteomics tools, most directly in a 2023 survey of mass-spectrometry approaches to the DDR that treats abundance, PTM, AP-MS, PL, and structural proteomics in parallel [17]. What has not been assembled is a synthesis organized around the specific biological problems of genome maintenance, a review that asks not "how does a labeling enzyme work?" but "what has PL taught us about the neighborhood of a break, a fork, or an R-loop, and what can it still uncover?" That is the gap this review addresses. We deliberately foreground biology over method: each section is built around a DDR problem, with the relevant PL chemistry introduced only insofar as it constrains what can be learned. Three problems in particular recur as unexploited yet tractable. They are the compositional core of DSB repair condensates, the immediate neighborhood of a DNA–protein crosslink, and a matched one-bait comparison of fork remodeling across distinct stresses, and we return to each as the review proceeds (Figure 1). We give correspondingly serious attention to limitations, because in the nucleus the difference between a genuine proximal partner and a labeling artifact is unusually easy to blur.

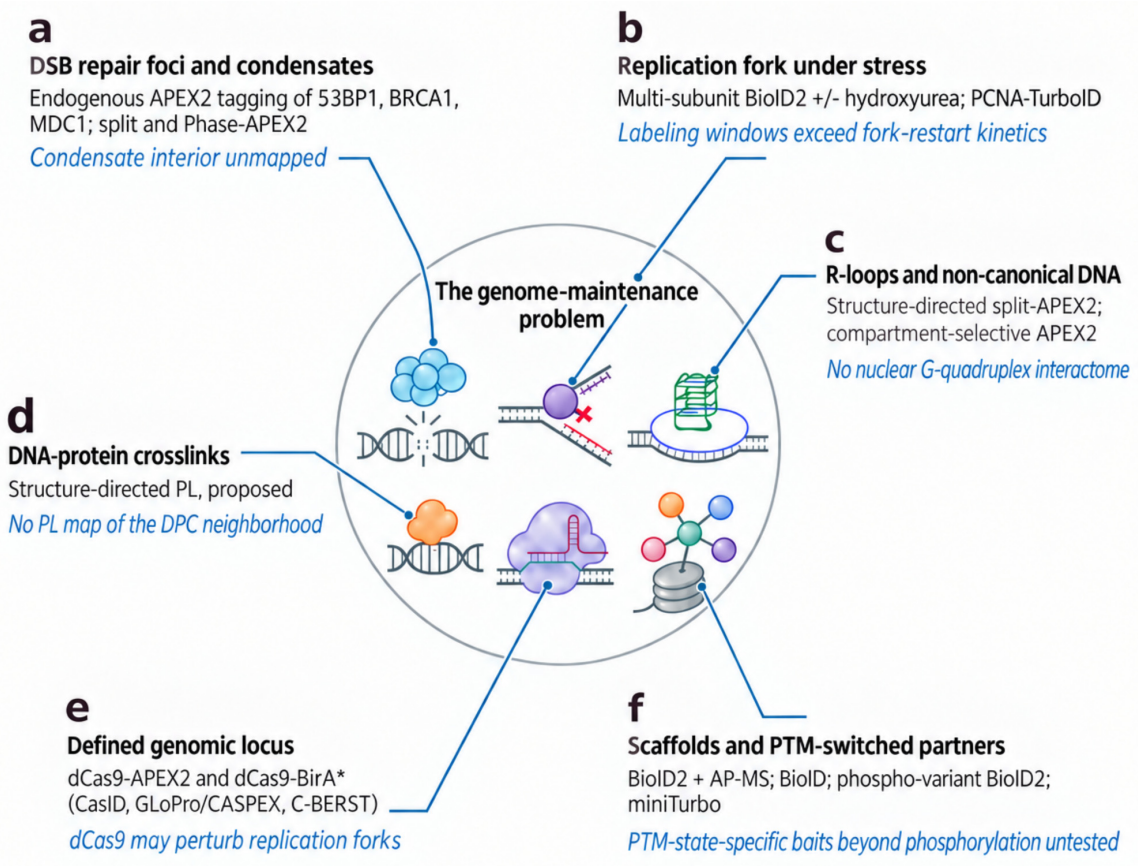

Figure 1. A problem-oriented map of proximity labeling in genome maintenance. Proximity-labeling strategies organized by the genome-maintenance problem they address (center, a nucleus containing representative lesions). For each problem the panel gives the PL approach, representative findings, and (in blue italics) the principal open gap. DSB repair foci and condensates: endogenous APEX2 tagging of 53BP1/BRCA1 and split/Phase-APEX2 designs [18]; APEX2 mapping of 53BP1/BRCA1/MDC1 discovered Shieldin [19], but the condensate interior remains unmapped. Replication fork under stress: multi-subunit BioID2 ± hydroxyurea and PCNA-TurboID reveal stress-dependent rewiring, including stress-enhanced ZPR1 and ANP32A associations [20] and damage-recruited PCNA responders [21,22]. R-loops and non-canonical DNA: structure-directed split-APEX2 and compartment-selective APEX2 define the m^{6}A-R-loop interactome [23] and mitochondrial G-quadruplex binders [24]. DNA–protein crosslinks (DPC): structure-directed PL is proposed, but no PL map of the DPC neighborhood yet exists; because the lesion is itself a protein, it is an ideal anchor for split/structure-directed labeling. Defined genomic locus: dCas9–APEX2/BirA* systems (CasID, GLoPro/CASPEX, C-BERST) map the locus-resident proteome [25–27], with the caveat that dCas9 may perturb replication forks [28]. Scaffolds and PTM-switched partners: BioID2 + AP-MS and BioID defined the SLX4 [29] and Ku [30] interactomes, and phospho-variant BioID2 the DSB-dependent TRIP12–Ku70 association [31], while the BLM–TOP3A–RMI1–RMI2 proximity map identified RAD54L2 [32]. BirA* denotes the promiscuous R118G mutant of bacterial BirA.

2. The Proximity Labeling Toolbox, Viewed from the Nucleus

Two enzyme families dominate (Figure 2, Table 1). Biotin ligases derive from bacterial BirA: BioID (BirA*) generates a reactive biotinoyl-5′-AMP that diffuses a short distance and reacts with accessible lysines, but requires long labeling windows of many hours [33]. BioID2 reduced the tag size and improved efficiency [34], and directed evolution of the ligase produced TurboID and miniTurbo, engineered biotin ligases that compress labeling to roughly ten minutes and thereby bring the technique within reach of DDR kinetics [35]; smaller and more active ligases have followed, among them ultraID [36]. Peroxidase-based APEX and its evolved successor APEX2 use hydrogen peroxide to convert biotin-phenol into a phenoxyl radical with

a sub-millisecond half-life, enabling labeling on the order of one minute and correspondingly sharp temporal resolution, at the cost of requiring exogenous H_2O_2 [37,38].

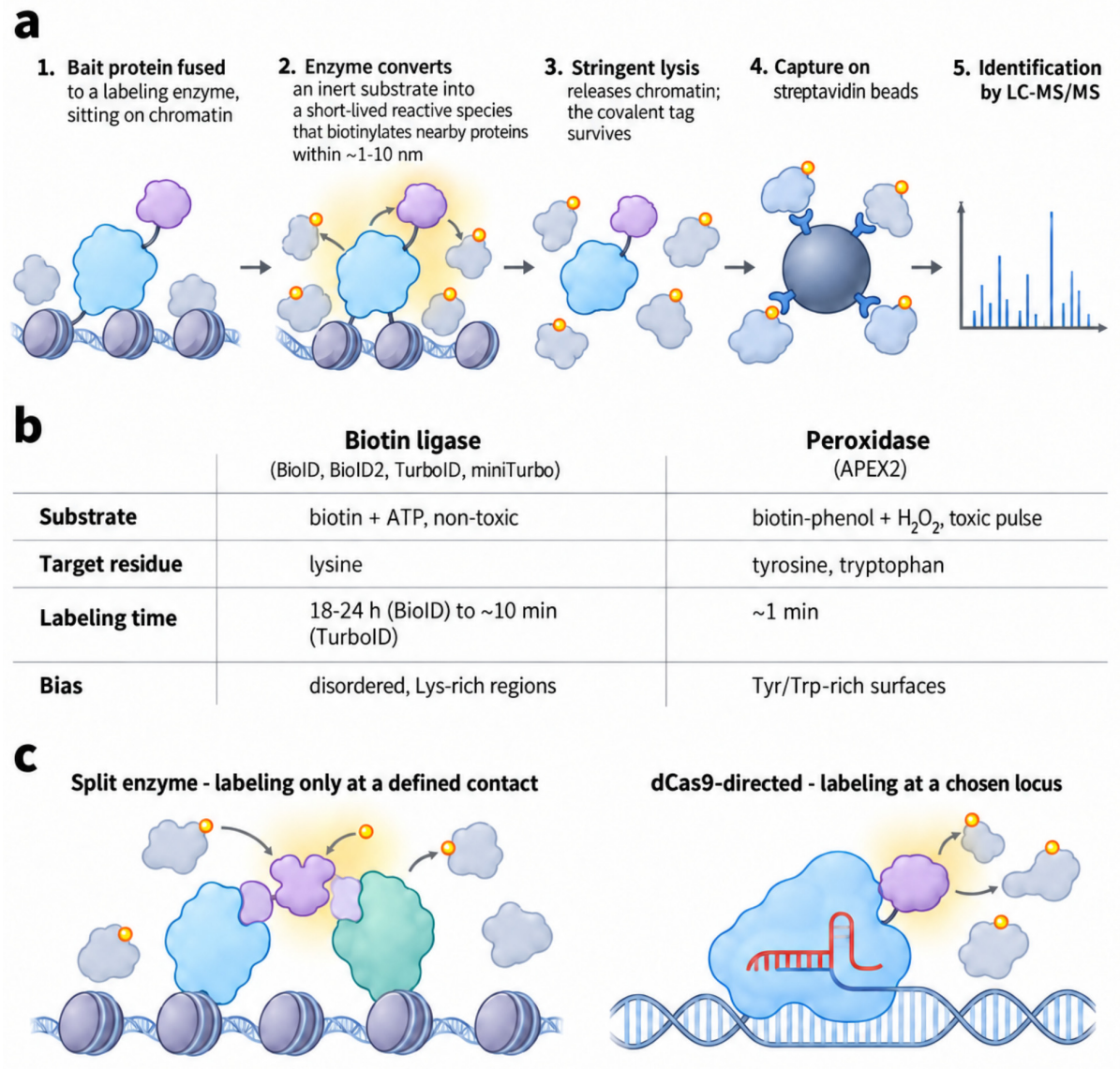

Figure 2. Proximity labeling chemistries and their fit to the DNA damage response. (**a**) General principle. A bait protein fused to a promiscuous labeling enzyme is expressed on chromatin (1); in living cells the enzyme converts an inert substrate into a short-lived reactive species that covalently biotinylates proteins within ~1–10 nm (2); because the tag is covalent it survives the stringent lysis needed to solubilize chromatin (3); biotinylated proteins are captured on streptavidin (4) and identified by LC–MS/MS (5). (**b**) The two dominant enzyme families. Biotin ligases (BioID, BioID2, TurboID, miniTurbo) use biotin (plus ATP), a non-toxic substrate, label lysine residues, and span labeling windows from ~18–24 h (BioID) to ~10 min (TurboID), with a bias toward disordered, lysine-rich regions. Peroxidases (APEX2) use biotin-phenol activated by a pulse of H_2O_2, label tyrosine and tryptophan, achieve ~1 min temporal resolution, and are biased toward Tyr/Trp-rich surfaces. Within this pair the practical differentiators for a DDR experiment are labeling time, substrate toxicity and target-residue chemistry; the labeled footprint differs more between these families and the newer photocatalytic chemistries than between the two families themselves. (**c**) Targeted configurations. Split enzymes reconstitute an active enzyme only where two fusion partners interact, turning PL into a contact-dependent test of a specific interaction or lesion; dCas9-directed systems tether the enzyme to a chosen genomic locus via a guide RNA to map the locus-resident proteome, with the caveat that dCas9 can perturb replication forks. Photocatalytic chemistries are omitted from this figure; they are compared in Table 1.

For DDR work, these differences are not cosmetic. The short labeling window of APEX2 and TurboID is what makes it feasible to capture the composition of a structure that exists for only a few minutes after damage, whereas classical BioID integrates over a period longer than the lifetime of most repair foci. The enzymes also differ in chemistry in ways that bias the recovered proteome: APEX-generated radicals react principally with electron-rich tyrosine and tryptophan residues, as site-level mapping of biotinylation events confirms [39], while biotin ligases target lysines and consequently favor proteins rich in intrinsically disordered, lysine-dense regions. A direct comparison of APEX2 and TurboID across cytosolic, nuclear, and membrane compartments confirmed that the two enzymes return overlapping but distinctly biased proteomes from the same compartment, and that part of the biotin-ligase bias is a downstream artifact of tryptic digestion at labeled lysines that can be partially mitigated by using an alternative protease [40]. The practical consequence for a DDR investigator is that enzyme choice should be treated as an experimental variable with biological consequences, not a matter of reagent availability. A bait studied with only one enzyme yields a systematically incomplete neighborhood.

A third development is contact-dependent labeling. Split versions of the enzymes, in which the biotin ligase or peroxidase is divided into two inactive fragments that reconstitute only when brought together by an independent interaction, convert PL from a neighborhood-mapping tool into a targeted validation tool: biotinylation occurs only where two specified proteins, or a protein and a defined nucleic-acid structure, coincide. Split-BioID established this principle for conditional monitoring of spatiotemporally defined complexes [41], a split-TurboID subsequently brought the same contact-dependent logic to the faster biotin-ligase chemistry [42], and directed evolution produced a split-APEX2 (sAPEX) with the kinetics of the peroxidase system [43]. Photocatalytic PL, which uses a localized light-activated catalyst to generate reactive intermediates with tunable and often shorter labeling radii, extends spatial precision further [44]. The approach was established by μMap, in which a photocatalyst anchored to an antibody maps protein microenvironments by Dexter energy transfer [45], and it has since been brought to chromatin by incorporating catalysts directly onto histone tails to read out chromatin-state changes [46]. These newer chemistries are the ones most likely to define the next decade of DDR interactomics, and they are almost entirely absent from earlier method catalogs written before their DDR applications appeared.

Table 1. Comparison of proximity labeling approaches for DNA damage-response studies.

Approach	Class	Labeling Time	Target Residue	Substrate/ Trigger	Distinguishing Feature	Representative DDR Use
BioID (BirA *)	Biotin ligase	18–24 h	Lys	Biotin + ATP (non-toxic)	First PL enzyme; integrates over hours, unsuited to fast events	Ku70 interactome [30]
BioID2	Biotin ligase	Several h	Lys	Biotin + ATP (low conc.)	Smaller (27 kDa), lower background	SLX4 scaffold map [29]; stressed replisome map [20]; Ku70 phospho-variant interactome [31]
TurboID	Biotin ligase	~10 min	Lys	Biotin + ATP	Fast enough for much of DDR biology; 35 kDa tag	PCNA damage interactome [21,22]
miniTurbo	Biotin ligase	~10 min	Lys	Biotin + ATP	28 kDa; less pre-biotin background, tighter temporal control	BLM–TOP3A–RMI1–RMI2 dissolvasome map (with BioID) [32]
APEX2	Peroxidase	~1 min	Tyr, Trp	Biotin-phenol + H_2O_2 (toxic)	Sharpest temporal resolution	Shieldin discovery [19]; NONO relocalization [47]

Table 1. *Cont.*

Approach	Class	Labeling Time	Target Residue	Substrate/ Trigger	Distinguishing Feature	Representative DDR Use
Split-BioID/sAPEX/split-TurboID	Split enzyme	Longer than parent (reconstituted activity is lower)	Lys/Tyr, Trp	As parent + interaction	Contact-dependent; validates a specific PPI or lesion	m^6A-R-loop mapping [23]; condensate core (Phase-APEX2; non-DDR proof of concept) [18]
Photocatalytic (e.g., µMap)	Photocatalyst	Light-gated (fast)	Varies	Light + probe	Tunable, often shorter radius; spatiotemporal trigger	Chromatin-state readout [46]
dCas9-directed (CasID/GLoPro–CASPEX/C-BERST)	Locus-targeted	Enzyme-dependent	Lys/Tyr, Trp	Biotin or biotin-phenol + H_2O_2, + sgRNA	Maps the proteome at a defined genomic locus	Locus-resident proteome [25–27]; damaged-locus mapping proposed (fork-perturbation caveat [28])

In-cell labeling radii for the core enzymes are broadly similar, experimentally on the order of ~1–10 nm in living cells [13,48]. These are experimentally estimated in-cell labeling radii, measured by molecular rulers and by spatial barcoding, and not intrinsic diffusion distances of the reactive intermediate. The available measurements place the biotin ligase and the peroxidase systems in the same approximate window and were not acquired under matched conditions, so a separate radius cannot be assigned to BioID, TurboID and APEX2 with confidence, because the measured distance also reports local protein density, residue accessibility and the lifetime of the reactive species. Within this group the practical differentiators for a DDR experiment are therefore labeling time, substrate toxicity and target-residue bias rather than footprint. Photocatalytic labeling is the one case in which a shorter and tunable radius is established. The labeling times given are the windows commonly used in published experiments and not universally applicable minima, since the sensitivity achieved in any particular experiment depends on substrate availability and uptake, bait expression level and localization, and the physiological state of the cell. A short window narrows the interval over which signal accumulates but does not provide an instantaneous record of composition, because labeling still integrates over that window and the recovered set is weighted by residence time within it. Section 8 treats both questions in full. BirA * denotes the promiscuous R118G mutant of bacterial BirA.

3. Double-Strand Break Repair Foci and Condensates

The best-known DDR application of proximity labeling is the mapping of DSB repair-factor neighborhoods, the first of the genome-maintenance problems compiled in Table 2. By tagging 53BP1, BRCA1, and MDC1 with APEX2 and combining labeling with quantitative mass spectrometry, Gupta and colleagues generated interaction neighborhood maps of these central repair factors and, in doing so, discovered Shieldin, a complex of three previously uncharacterized subunits (SHLD1–3) together with the known resection inhibitor REV7, as a downstream effector of the 53BP1–RIF1 axis that restrains end resection and sensitizes BRCA1-deficient cells to PARP inhibitors [19]. Shieldin was identified concurrently by several groups using genetic screens [49–51]; REV7 had already been placed downstream of 53BP1–RIF1 as an inhibitor of end resection [52], and the 53BP1–RIF1 axis itself had been defined earlier [53]; that independent routes converged on the same complex within months indicates that the proximity map was reading functional biology rather than returning a list of co-residents. The significance of this study is twofold. First, it demonstrated that PL applied to endogenous DDR baits could reveal not just known partners but an entirely new functional complex with direct therapeutic relevance. Second, it validated the core premise that spatially resolved, in-cell labeling recovers repair interactions that had escaped years of conventional biochemistry.

Table 2. Genome-maintenance problems addressed by proximity labeling: representative studies and open gaps. BirA * denotes the promiscuous R118G mutant of bacterial BirA.

DDR Problem	PL Strategy	Representative Study	What PL Revealed/Could Reveal
DSB repair-factor neighborhoods	Endogenous APEX2 tagging of 53BP1/BRCA1/MDC1	Gupta et al. 2018 [19]	Shieldin as a new 53BP1 effector; PARPi-sensitivity link
DSB condensate interior	Multi-input split, AND-gate (Phase-APEX2)	Chen et al. 2025, preprint [18]	Core vs. client composition, unmapped at DSBs
Replisome under stress	Multi-subunit BioID2 ± hydroxyurea	Jurkovic et al. 2024 [20]	Stress-dependent rewiring; ZPR1–ASF1B/POLE4, ANP32A–POLE4
Damage-recruited fork proteome	PCNA–TurboID + oxidative damage	Rona et al. 2024 [21]; protocol [22]	MMR access to PCNA restricted by D-type cyclins; BER factors at oxidative lesions
R-loop microenvironment	Structure-directed split-APEX2	Zhu et al. 2025 [23]	m^6A-R-loop interactome; ZC3H4 and CCDC124 at virus-induced R-loop granules
Non-canonical DNA (G-quadruplex)	Compartment-selective APEX2	Wang et al. 2025 [24]	Mitochondrial G4-binding proteins
DPC/topoisomerase cleavage complex	Structure-directed PL (proposed)	None	Open: no PL map of the DPC neighborhood exists
Defined genomic locus	dCas9–APEX2/BirA * (CasID, GLoPro, C-BERST)	Schmidtmann 2016 [25]; Myers 2018 [26]; Gao 2018 [27]	Locus-resident proteome
Repair-scaffold partners	BioID/BioID2/miniTurbo + AP-MS	Aprosoff 2023 [29]; Abbasi 2019 [30]; Ho 2025 [32]	Comprehensive SLX4/Ku interactomes; RAD54L2 at the BLM dissolvasome
PTM-switched recruitment	Phospho-variant BioID2	Abbasi et al. 2023 [31]	TRIP12 as a DSB-dependent Ku70 partner

This success also points to the frontier that remains open. DSB repair factors do not merely bind partners; they organize into micron-scale foci with the physical properties of biomolecular condensates [54]. The 53BP1 assembles chromatin domains that behave as liquid-like compartments, undergoing fusion and fission and depending on multivalent, phase-separation-prone interactions to concentrate effectors and shield DNA ends [55]. Whether these compartments are true liquid condensates or chromatin-tethered clusters remains contested; super-resolution imaging argues that 53BP1 is organized into nanodomains whose shape is set by chromatin topology rather than by demixing [56], so a core-versus-client measurement would test the condensate model rather than presuppose it. These condensates are nucleated in part by damage-induced non-coding RNAs transcribed at break sites by an RNA polymerase II pre-initiation complex, without which mature DDR foci and 53BP1 condensates fail to form [57]. Condensation is a broader theme in the DDR than 53BP1 alone [58]: MRNIP forms droplets that concentrate the MRN complex to accelerate break sensing and end resection [59], and poly(ADP-ribose) synthesized at damage sites seeds the liquid demixing of intrinsically disordered proteins at damage sites [60], including the transient accumulation of FUS into PARG-reversible compartments [61]. An in silico survey of 533 Gene Ontology–annotated DNA-repair genes predicted 56 (~10%) to be highly disordered (PONDR VSL2 > 0.7), and a subset of these, MRNIP among them, forms liquid-like condensates in cells [59]; whether 10% exceeds the rate for the proteome at large under the same threshold has not been established, so the figure nominates candidates rather than demonstrating that repair proteins are unusually condensation-prone. The

internal proteome of these compartments, meaning which proteins are enriched inside a 53BP1 or BRCA1 condensate rather than merely nearby in the nucleoplasm, is exactly the kind of question that imaging cannot answer and that neighborhood-resolved labeling is positioned to address.

At DSB repair condensates specifically, this remains largely unexplored. Proximity labeling has begun to enter condensate biology more broadly, and an APEX2-based approach recently reconstructed the dynamic FUS interactome across its liquid–liquid phase transition in living cells [62]. Such studies have targeted model or stress-granule condensates rather than damage-induced repair compartments, and the technical reason DSB condensates lag is instructive: standard single-bait APEX2 or TurboID cannot by itself distinguish the condensed phase from the surrounding dilute nucleoplasm, because its labeling radius spans both. The emerging solution is multi-input, contact-dependent labeling. A recently described Phase-APEX2 strategy, so far reported only in a preprint, combines a split peroxidase with a light-controlled peroxide generator in an AND-gate configuration, so that rapid labeling is confined to the crowded interior of a condensate and amplified relative to the dilute phase; applied to nucleoli and stress granules, it resolved core membraneless-organelle proteomes that single-input methods missed [18]. Transplanting this logic to DSB repair condensates, so as to define the compositional core of a 53BP1 or BRCA1 compartment and how it changes with repair pathway choice, cell-cycle phase or therapeutic perturbation, is in our assessment among the most tractable unexploited applications of PL in DSB biology. The peroxidase chemistry carries a liability here that it does not carry at a nucleolus or a stress granule: generating peroxide inside the compartment delivers an oxidant onto the very chromatin being profiled, where it yields the oxidative lesions that recruit base-excision-repair factors and activate PARP (Section 8), so the measurement risks creating part of the neighborhood it reports. A generator-inactive arm and a light-off arm at matched expression are the minimum controls, and an AND-gate assembled from split biotin ligases would avoid the oxidant altogether.

4. The Replication Fork and Replisome Under Stress

Replication forks present a distinct challenge: the replisome is a moving, compositionally dynamic machine whose accessory factors change as it encounters obstacles, and mammalian cells lack the defined origin sequences that would allow locus-based capture. Historically, isolation of proteins on nascent DNA (iPOND) addressed this by pulse-labeling newly synthesized DNA with a nucleotide analog and recovering the associated proteins, providing a nascent-chromatin-centered view of fork proteomes [63]. Proximity labeling offers a complementary, bait-centered view that reports on the neighborhood of a chosen replisome subunit in living cells, including transient and low-abundance factors that nascent-DNA capture may miss.

A comprehensive recent application defined the proximal interactomes of seventeen replisome components spanning replication protein A, chromatin remodelers, polymerases, and the CMG helicase, using BioID2, and then asked how these neighborhoods are remodeled by replication stress [20]. Hydroxyurea-induced fork stalling modulated 108 nuclear protein associations, 45 of them enriched and 63 depleted, and redistributed a further eleven proximal proteins among baits, a direct, proteome-scale readout of how the fork rewires its associations under stress. The study surfaced poorly characterized factors, including stress-enhanced associations of ZPR1 with ASF1B and POLE4 and of the histone-acetylation regulator ANP32A with POLE4, each confirmed independently by proximity ligation assay, illustrating the value of following multiple subunits of the same complex to build internal confidence. In a focused counterpart, fusing PCNA to TurboID and inducing oxidative damage in G1-synchronized cells captured the chromatin-bound PCNA neighborhood

and showed that D-type cyclins restrict the access of mismatch-repair proteins to PCNA; a parallel TurboID experiment on cyclin D1 itself enriched base-excision-repair factors specifically, the only repair pathway significantly over-represented in that neighborhood [21]. A companion protocol establishes the approach as a generalizable route to identifying DNA damage responders [22]. Together these studies show that PL can turn the replisome from a structure studied one interaction at a time into a system whose stress response is mapped in a single experiment.

What emerges from placing these studies side by side is that different genotoxic stresses should remodel the fork neighborhood in mechanistically distinct, and in principle distinguishable, ways, and that this stress-specificity is itself the most informative and least exploited dimension of the approach. Nucleotide depletion by hydroxyurea drives single-stranded DNA accumulation and a corresponding enrichment of replication protein A and its regulators [20], and with prolonged exposure drives fork reversal and collapse [64]; oxidative lesions enrich base-excision-repair factors around a lesion-recruited bait while remodeling which mismatch-repair proteins engage PCNA [21]; and replication-blocking DNA–protein crosslinks reorganize the fork when it collides with a persistently trapped protein, triggering the replication-coupled repair we take up in Section 5. Each of these represents a different reorganization of the same molecular neighborhood, yet they have been studied in separate systems with separate baits, so the field lacks a controlled, PL-based comparison of how one replisome subunit's interactome differs across stresses. Nascent-DNA capture has already delivered matched comparisons of this kind [65], so the case for a bait-centered panel rests on what it adds rather than on novelty: transient factors that never reach nascent DNA, and neighborhoods resolved by subunit rather than by lesion. Such a comparison, using one bait, several defined insults and matched labeling windows, would convert anecdotal differences into a systematic map of fork stress responses. The equivalent comparison between drug-sensitive and drug-resistant backgrounds remains similarly unexplored.

5. Structure-Specific Lesions: R-Loops, Non-Canonical DNA, and DNA–Protein Crosslinks

Beyond breaks and forks, PL is increasingly targeted at specific lesion structures whose associated proteomes are otherwise inaccessible. R-loops, which are three-stranded RNA–DNA hybrids with a displaced single strand, are potent sources of transcription–replication conflict and genome instability [66], and their protein environments are difficult to isolate because the structures are transient and sequence-dispersed. A chemically inducible split-APEX2 system for R-loops exemplifies how modern PL chemistry can be engineered around a lesion: dual recognition, using the RNA–DNA hybrid-binding domain of RNase H1 to mark R-loops [67] and an m^6A-reader YTH domain to require an epitranscriptomic mark [68], restricts enzyme reconstitution to modified R-loops, and an inducible dimerization module amplifies signal. Applied in living cells, this approach mapped the spatial distribution of m^6A-modified R-loops; in herpes simplex virus-infected cells, where these structures accumulate in phase-separated granules inside viral replication compartments, it nominated two host factors not previously connected to these structures, the transcription-restriction factor ZC3H4 and the ribosome-associated protein CCDC124, as regulators of those granules [23]. The demonstration is therefore a proof of principle in a viral rather than a DDR setting, but the design principle generalizes directly, which is to combine a structure-selective domain with a split enzyme so that labeling reports on a defined lesion rather than on a bait protein. The same strategy has been extended to non-canonical DNA structures: a compartment-selective APEX2 approach was used to identify proteins

bound to mitochondrial G-quadruplexes, a class of structure with its own links to genome instability [24].

Damage-responsive relocalization can itself be exploited. NONO is a paraspeckle-associated RNA-binding protein of the DBHS family that redistributes after DNA damage, which is what makes it an informative bait. A stably expressed NONO–APEX2 fusion reproduced the endogenous behavior of NONO, including its increased nucleolar localization after DNA damage, and biotinylated paraspeckle proteins in vivo, demonstrating that PL can track a factor's changing neighborhood as it redistributes in response to genotoxic stress [47].

A conspicuous gap in this landscape is the DNA–protein crosslink (DPC). DPCs, which include trapped topoisomerase cleavage complexes and covalently trapped methyltransferases as well as non-enzymatic adducts from aldehydes and platinum drugs, are among the most cytotoxic lesions, because a bulky protein covalently fixed to DNA blocks replication and transcription [69,70]. Their repair hinges on which proteolytic and downstream activities reach the trapped protein: the replication-coupled protease SPRTN and the proteasome act as independent DPC proteases with distinct substrate preferences [69,71], and for trapped topoisomerases both proteasomal and non-proteasomal routes contribute to debulking [72], additional proteases including FAM111A [73], the yeast aspartic protease Ddi1 [74], and the SUMO-targeted ACRC/GCNA family [75] have since been implicated, poly(ADP-ribosyl)ation marks certain DPCs for removal [76], the p97/VCP ATPase extracts trapped PARP1 from chromatin [77], and a transcription-coupled route depends on the Cockayne syndrome proteins [78]. Not every route is proteolytic: the tyrosyl-DNA phosphodiesterases TDP1 and TDP2 hydrolyze the phosphotyrosyl bond that tethers a trapped topoisomerase to DNA [79], a reaction that for topoisomerase 2 is licensed by SUMO2 conjugation through the ligase ZATT [80], and selective autophagy of DNA lesions provides a further clearance route [81]. This is a repair problem defined almost entirely by the local protein environment of the lesion, which is precisely what proximity labeling is built to resolve, yet the immediate neighborhood of a DPC or a specific topoisomerase cleavage complex has not, to our knowledge, been mapped by PL in cells, although extract-based chromatin proteomics has followed repair-factor assembly on crosslinked templates [82]. Because the lesion is itself a protein, a split or structure-directed labeling scheme anchored on the trapped species is conceptually feasible and would convert an inventory of candidate DPC proteases into a spatially resolved, in-cell map of which factors actually assemble at the crosslink.

6. Locus-Directed Proximity Labeling

The applications above tether the enzyme to a protein bait. An alternative is to tether it to a genomic locus using catalytically dead Cas9 (dCas9), so that a single guide RNA directs labeling to a chosen site. Locus proteomics predates proximity labeling: hybridization capture of a repetitive locus with a nucleic-acid probe defined the telomeric proteome [83]. The original CasID fused dCas9 to BirA* and validated locus-proximal labeling at repetitive telomeric and satellite sequences, identifying known and novel locus-associated proteins [25,84]. Because the slow kinetics of first-generation biotin ligases limited specificity, subsequent systems fused dCas9 to the faster APEX2, developed independently as GLoPro/CASPEX and as C-BERST, improving speed, temporal control, and signal-to-noise at defined loci [26,27]. Guide-RNA tiling across a target increases enzyme density and reduces off-target noise [26]. A complementary route dispenses with dCas9 altogether and aims the enzyme with an antibody: Protein A–APEX2 fusions directed against a histone modification label the proteome surrounding that mark, trading sequence specificity for chromatin-state specificity [85]. An engineered chromatin reader fused to a biotin ligase

reaches the same end genetically and has been used to profile the protein interactome at defined histone marks [86], which is the configuration closest to a DDR application: a reader for a damage-induced mark would report the proteome assembled on it.

For DDR research, locus-directed PL is attractive because it could, in principle, map the proteome that assembles at a defined, inducibly damaged site rather than at breaks distributed unpredictably across the genome, pairing the technique with the site-specific nuclease systems that already underpin break-proximal chromatin profiling [87] or with defined fragile loci. A quantitative ceiling tempers this: the dCas9 systems were validated at repetitive targets, where many enzyme copies accumulate, whereas a single inducible break presents one or two copies per nucleus, so guide tiling or multi-site induction is likely to be required. A critical caveat tempers this promise: dCas9 binding is not inert. In budding yeast, dCas9 impedes replication fork progression and, when targeted to a tandem-repeat array, provokes fork stalling and contraction of the array [28]; dCas9-induced R-loops are themselves mutagenic, generating base substitutions on the displaced strand at a frequency of roughly 10^{-5} [88]. Whether these effects are as pronounced in mammalian cells has not been established, but the mechanism, a stably bound protein and a persistent R-loop at the target, is not organism-specific. In a DDR experiment, where the readout is itself the damage-associated proteome, a targeting reagent that perturbs replication and generates local instability is a serious confounder that must be controlled for explicitly, for example, with catalytically matched non-targeting guides and orthogonal damage induction. Locus-directed PL is powerful but, in the damage context, uniquely prone to reporting on artifacts of its own targeting.

7. Deconstructing Repair Scaffolds

Large scaffold proteins that nucleate multiple, context-dependent complexes are ideal PL subjects because their transient and combinatorial partners are poorly served by single-shot AP-MS. The Fanconi-anemia-associated endonuclease scaffold SLX4 illustrates the point: despite its central role in homologous recombination and its dependence on binding and activating the structure-selective endonucleases SLX1, MUS81–EME1, and XPF–ERCC1, a comprehensive catalog of its partners had never been reported. Combining BioID2 with AP-MS yielded 156 and 81 high-confidence proximal proteins, respectively, a combined set dominated by novel partners, and revealed associations beyond canonical repair, including chromatin remodeling and RNA metabolism, that suggest underappreciated scaffold functions [29]. The pairing of the two methods in that study is instructive. Only 16 proteins were detected by both, so each method recovered a large set that the other missed, which argues against treating any single interaction method as complete.

The Ku70/Ku80 heterodimer, the DNA-end sensor of non-homologous end joining, offers a second and methodologically richer illustration. A first BioID/AP-MS map of Ku70 defined a comprehensive interaction landscape extending well beyond canonical end-joining partners [30]. A follow-up study then exploited a strength unique to proximity labeling: by comparing BioID2 neighborhoods of wild-type Ku70 against a phosphomimetic (S155D) and a phosphoablative (S155A) variant, it isolated proximal proteins that depend on a specific phosphorylation state, identifying the E3 ubiquitin ligase TRIP12 as a Ku70 partner recruited in response to double-strand breaks and validating the association by proximity ligation assay and co-immunoprecipitation [31]. The limitation of the design belongs beside its logic: aspartate is a charge mimic, not phosphoserine, and the BRCT, FHA and 14-3-3 modules that read damage-induced phosphorylation frequently fail to bind S → D substitutions, so a phosphomimetic comparison can miss the very interactions it is built to find unless it is checked against the endogenous modified site. This phospho-state-resolved design directly addresses the PTM-driven, transient recruitment that defines much of the DDR and that stable-complex purification cannot resolve, and it is a template that could be applied to

any repair factor whose engagement is switched by a defined modification. A more recent BioID- and miniTurbo-based proximity map of the BLM–TOP3A–RMI1–RMI2 dissolvasome extended the same approach to the homologous-recombination machinery, charting the neighborhood of this genome-stability scaffold and identifying RAD54L2, an SNF2-family ATPase, as a previously unrecognized suppressor of sister-chromatid exchange [32].

The general lesson is that a proximity map is likely to be more complete than a stable-complex purification for any DDR factor that acts as an organizing center, assembling different complexes at different lesions, cell-cycle phases or PTM states, provided it is interpreted with the caveats discussed next.

Read across these studies, the comparisons in which the bait or the target locus is held constant are the only ones that speak to method performance, and there are four of them. On SLX4, BioID2 and affinity purification returned 156 and 81 high-confidence proximal proteins with 16 in common [29]. On Ku70, proximity labeling and affinity purification shared 22 proteins and 27 were retained after scoring [30]. On BLM, tagging with miniTurbo at the N terminus and at the C terminus returned 51 and 15 proximal proteins [32]. At telomeres, dCas9-directed APEX2 recovered 387 and 359 enriched proteins in two independent studies [26,27], while only 18 proteins were common to C-BERST, proximity biotinylation and hybridization capture at the same locus [27]. The consistent result is that the choice of method, and even the position of the tag on the same bait, changes the identity of the recovered set more than it changes its size. Partial overlap is therefore the expected outcome rather than a failure of either method and no single approach should be read as a complete account of a neighborhood. A comparison across studies that do not share a bait would not support the same inference, because bait, compartment, cell line, scoring model and threshold all differ, so any intersection would measure those differences rather than the labeling chemistry. Side-by-side benchmarks acquired under matched conditions by the groups that engineered these enzymes remain the appropriate basis for comparing their efficiency [13,35], and in practice the dominant costs of a proximity-labeling experiment are instrument time and the labeling scheme rather than the enzyme itself.

Three further observations emerge when these maps are read together rather than one at a time. First, the proteins that recur across unrelated baits are dominated by abundant chromatin, nucleolar and ribonucleoprotein species, which is the signature of the abundance and accessibility bias analyzed in Section 8 rather than evidence of shared biology, and it is why contaminant repositories are the standard control in this field. Second, where the primary authors performed network clustering, the functional categories recovered are strikingly consistent across different baits and different enzymes. DNA repair and replication, chromatin remodeling and modification, chromosome structure and dynamics, and RNA splicing and processing recur in the SLX4, Ku70 and dissolvasome maps alike [29,30,32], which supports the inference that genome-maintenance scaffolds sit at the interface between repair and RNA metabolism more consistently than any single-bait study could establish. Third, in every case the mechanistic advance that followed came from one protein extracted from a large list by orthogonal validation, Shieldin from the 53BP1 network [19], TRIP12 from the phospho-resolved Ku70 comparison [31] and RAD54L2 from the dissolvasome map [32]. We have not merged these datasets into a single network, because lists built under incompatible thresholds and scoring models would generate apparent edges that no individual study supports.

8. Limitations and Interpretive Caveats

The credibility of a PL dataset in the nucleus rests on how well its systematic biases are understood and controlled. Five systematic biases are paramount (Figure 3); two further issues cut across all five and are taken up afterwards, namely how a candidate is called and which molecular form of a protein the identification actually stands for.

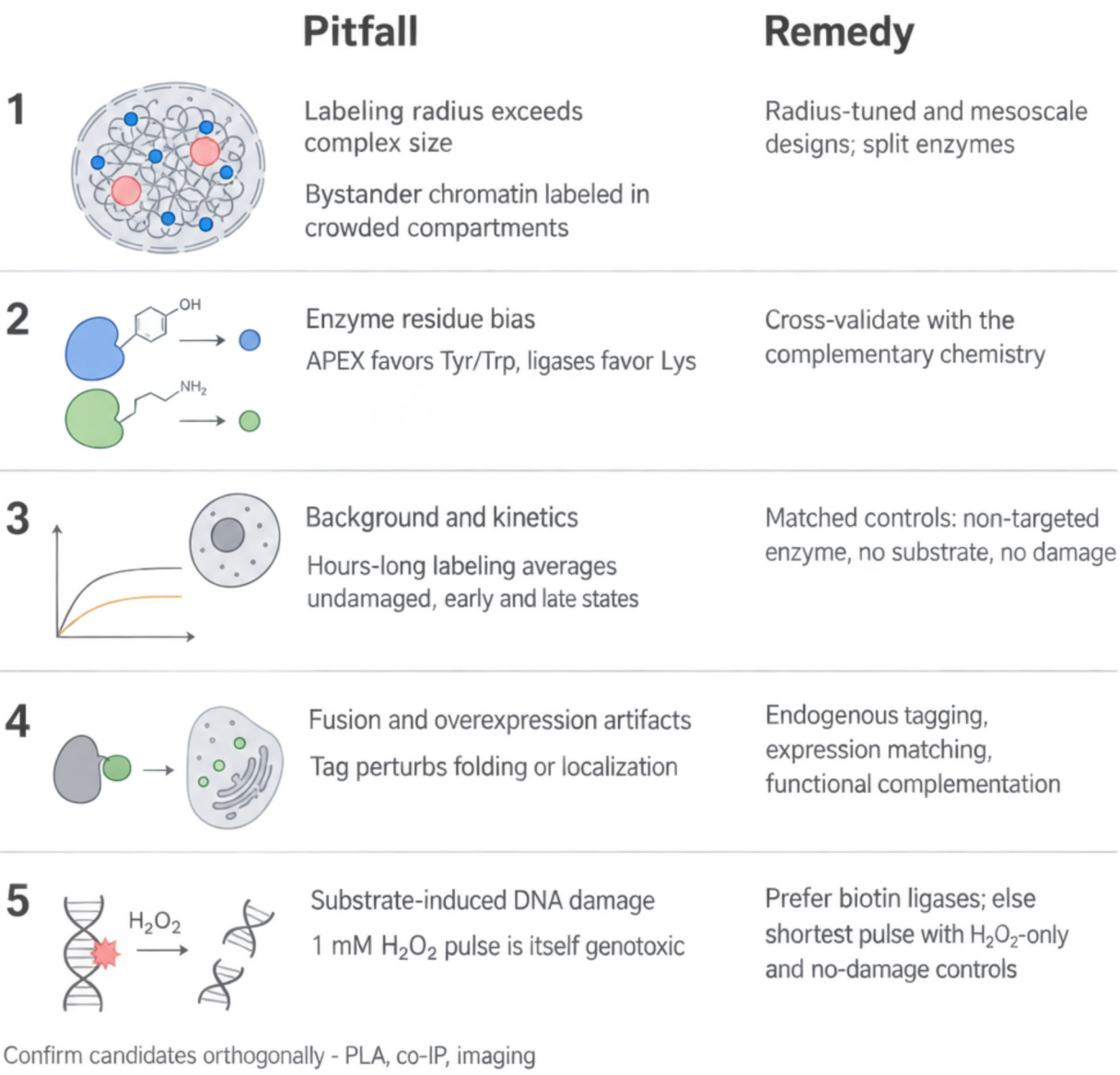

Figure 3. Interpreting proximity labeling in the nucleus—pitfalls and paired controls. Five systematic biases of nuclear PL (**left**, "Pitfall") paired with the controls that address them (**right**, "Remedy"). (1) Labeling radius versus chromatin compaction: a reactive radius larger than individual complexes labels bystander chromatin in crowded compartments, so an apparently enriched protein may merely co-reside; radius-tuned and mesoscale designs and split enzymes restrict labeling to a defined contact. (2) Enzyme residue bias: APEX favors Tyr/Trp and biotin ligases favor Lys, so residue-poor proteins are under-labeled and wrongly scored absent; cross-validate with the complementary chemistry and take the union of the two enzymes' coverage. (3) Background and kinetics: endogenous biotinylation creates background and an enzyme integrating over hours averages the undamaged, early and late states of a focus whose recruitment steps are ordered within minutes; subtract matched controls (non-targeted enzyme, no-substrate, no-damage), match the labeling window to the event, and keep temporal claims conservative. (4) Fusion and overexpression artifacts: a bulky tag or non-physiological expression can perturb folding or localization and create neighborhoods the endogenous protein never samples; use endogenous tagging, expression-level matching and functional complementation tests. (5) Substrate-induced DNA damage (peroxidase systems): the 1 mM, one-minute pulse of H_2O_2 required for APEX2 labeling is itself genotoxic and can superimpose a substrate-evoked oxidative-stress proteome onto the DDR; prefer biotin-ligase systems when sub-minute resolution is not essential, otherwise use the shortest effective H_2O_2 pulse with matched H_2O_2-only and no-damage controls. Across all five, candidates should be confirmed orthogonally (PLA, co-IP, imaging), since the mass-spectrometry list is not the endpoint.

First, labeling radius versus chromatin architecture. There is no single labeling radius. The reactive intermediates act over distances on the order of one to ten nanometers in cells. That figure is an experimentally estimated labeling radius derived from molecular-ruler measurements at the nuclear pore [89] and, more recently, from spatial barcoding [48], rather than from any single kind of experiment [13], and it is not the intrinsic diffusion distance of the reactive intermediate. It corresponds to the scale of a single nucleosome and is smaller than many repair assemblies, so the problem is not that the footprint exceeds a complex but that, inside a compartment hundreds of nanometers across, nothing in the chemistry separates a functional neighbor from a co-resident. Standard APEX2 and BioID therefore struggle to distinguish a chromatin-specific environment from the bulk nuclear proteome, a limitation that has motivated radius-tuned and mesoscale designs, which trade resolution at the level of a single complex for a reading of chromatin-domain occupancy, such as MesoMap [90]. In a foci- and condensate-organized nucleus, an apparently enriched protein may simply be a co-resident of the same crowded compartment rather than a functional partner. Recent spatial-barcoding measurements complicate the simple radius picture further: TurboID appears to label largely through direct contact with its targets rather than by free diffusion across a fixed radius, while APEX2 combines efficient contact labeling with a lower-level diffusive component, so a single nominal labeling radius can understate how strongly the recovered neighborhood depends on enzyme chemistry and physical contact [48]. Because these measurements were not acquired under conditions matched across the enzyme families, a separate effective radius cannot be assigned to BioID, TurboID and APEX2 with confidence.

Second, enzyme residue bias. As noted, APEX radicals favor tyrosine and tryptophan while biotin ligases favor lysine-rich, disordered regions, and the digestion step compounds these biases [40]. A protein poor in the preferred residues can be systematically under-labeled and wrongly scored as absent; conversely, disordered, lysine-dense repair factors may be over-represented in biotin-ligase datasets. Cross-validation with the complementary enzyme chemistry, rather than reliance on a single system, is the appropriate control.

Third, background and kinetics. Endogenous biotinylated carboxylases and non-specific labeling generate a background that must be subtracted using rigorously matched controls, namely non-targeted enzyme, no-substrate and no-damage conditions. More subtly, labeling time must be reconciled with the speed of the process under study: repair foci persist for hours, but the recruitment steps that build them are ordered over seconds to minutes, so an enzyme that integrates over hours returns one average of the undamaged, early and late states rather than any one of them, and even ten-minute TurboID labeling blurs the earliest signaling events. Temporal interpretation should be explicit and conservative.

Fourth, overexpression and fusion artifacts. The enzyme fusion, which for TurboID is roughly 35 kDa, can perturb the localization, folding, or function of the bait, and non-physiological expression can create neighborhoods that the endogenous protein never samples. Endogenous tagging, expression-level matching to the native protein, and functional complementation tests are the safeguards.

Fifth, and specific to this field, substrate-induced damage. The peroxidase systems require exogenous hydrogen peroxide, which is itself a genotoxic oxidant: it produces oxidative base lesions and single-strand breaks, activates PARP, and engages the very damage response under study [91]. The relevant thresholds are low and the kinetics fast: in macrophages, H_2O_2 at 40 μM already inhibited DNA synthesis and generated single-strand breaks in under thirty seconds, with poly(ADP-ribose) polymerase activated over the same concentration range and NAD^+ depleted as a consequence [92]. Substrate-induced damage therefore begins well inside the one-minute window in which APEX2 labeling itself takes place. Using APEX2 to profile the DDR therefore risks superimposing a substrate-evoked

oxidative-stress proteome onto the biology of interest, and the 1 mM, one-minute pulse of H_2O_2 that standard APEX2 protocols require [37,38,93] is difficult to separate cleanly from a physiological signal, the more so because proximity-labeling protocols in this very field use H_2O_2 at 250 µM, a quarter of the labeling dose, precisely to inflict the oxidative lesions under study [22]. Where sub-minute temporal resolution is not essential, biotin-ligase systems avoid this particular confounder; where APEX2 is preferred for its speed, rigorously matched H_2O_2-only and no-damage controls and the shortest effective peroxide exposure are indispensable, and interpretation should acknowledge that part of the labeled neighborhood may reflect the response to the labeling reaction itself.

Underlying all of these biases is how a candidate is called in the first place. A PL neighborhood is a quantitative comparison rather than a binary list. Enrichment over matched controls must be scored statistically, using SAINT- [94] or CompPASS-style [95] probabilistic models or defined fold-change and false-discovery thresholds across biological replicates, and the quantification strategy, whether label-free, TMT or SILAC, should be stated alongside it. Effect size and significance are not interchangeable. A proximity-labeling comparison needs both an estimate of enrichment and a multiplicity-corrected significance estimate, and probabilistic scoring against matched and repository controls is the field standard because the null distribution inside a crowded nuclear compartment is not the one a simple fold-change cut off assumes. Recovery also scales with abundance, accessibility and residence time rather than with functional importance, so nuclear datasets are reliably dominated by the same highly abundant chromatin, nucleolar and ribonucleoprotein species; contaminant repositories assembled from large numbers of unrelated purifications are the standard control [96]. Thresholds set too loosely turn a crowded nuclear compartment into a long list of spurious candidates; set too tightly, they discard the weak, transient partners the method exists to capture. Stating the scoring model and its cutoffs is part of making a nuclear PL dataset interpretable, not a downstream formality.

A further limitation concerns resolution in the protein dimension rather than the spatial one. Bottom-up PL workflows identify protein groups from tryptic peptides, so digestion severs the connectivity between modifications carried on the same molecule and leaves a peptide-to-protein inference problem [97]; a neighborhood is therefore reported as a list of gene products rather than of the particular proteoforms actually present at the lesion, a proteoform being one of the distinct molecular forms a single gene gives rise to, including every combination of post-translational modification [98,99]. The scale of that gap is not marginal: the number of distinct human proteoforms is thought to exceed the number of protein-coding genes by orders of magnitude, although the true figure remains unsettled [100]. This matters more in the DDR than in most compartments, because the interactions being mapped are defined by post-translational modification: the proteoform recruited to a break is frequently not representative of the bulk population of that protein in the nucleus. For one enzyme family, the chemistry may compound the problem, because the residue that carries the mark is the residue the enzyme labels. A lysine already carrying ubiquitin, acetyl or SUMO offers no free ε-amine to a biotin ligase, and a phosphorylated tyrosine, whose phenolic hydroxyl is esterified, should be close to unreactive toward a phenoxyl radical. For a protein presenting tens of accessible lysines, this is unlikely to change whether the molecule is captured, since one adduct anywhere on it suffices; the effect should matter where modification is stoichiometric and multi-site, as in polyubiquitin chains, hyper-SUMOylation and lysine-dense disordered segments, and there a modified proteoform would be under-recovered precisely where its modification is functionally decisive. The argument bears on lysine marks and biotin ligases far more than on APEX2, whose Tyr/Trp chemistry is largely orthogonal to the Ser/Thr-directed phosphorylation that dominates damage signaling. To our knowledge, none of this has been

measured; it is straightforward to test with synthetic modified peptides and deserves to be quantified. Designs that interrogate proteoforms directly are therefore valuable beyond their immediate biological result: comparing the BioID2 neighborhoods of phosphomimetic and phosphoablative Ku70 [31] is a charge-mimic proxy for a proteoform-resolved interactome, and the same logic applied to ubiquitin- or SUMO-locked variants would move PL from a protein-level toward a species-level map of the damage response. Three routes toward proteoform-resolved proximity labeling are worth distinguishing, because they differ in how much new technology they require. The first needs none. Modification-locked bait variants interrogate one proteoform at a time by construction, the phosphomimetic and phosphoablative Ku70 comparison [31] being the existing example and ubiquitin- or SUMO-locked variants the obvious extension, and reader-domain targeting does the same from the other direction: tethering the enzyme through a domain that binds a specific mark, as ChromID does for chromatin states [86], conditions the entire readout on the presence of that mark. Neither resolves proteoforms in the output, but both make the input proteoform-defined, which is enough to answer most mechanistic questions in the DDR. A second route is measurement rather than design: enriching biotinylated peptides with anti-biotin antibodies [39] reports which residues were actually labeled, and applying established PTM-enrichment chemistries to a proximity-labeling eluate would report which modified forms were present in the neighborhood. These are available now and would convert the residue- and modification-bias arguments made above from chemistry into data. The third route is the genuinely hard one: reading the eluate at the level of intact protein species rather than tryptic peptides [97]. Its obstacles are specific and addressable. They are the near-irreversibility of the streptavidin–biotin interaction, which makes intact labeled proteins difficult to release under conditions an intact-protein workflow tolerates, and the variable number of biotin adducts per molecule, which turns one proteoform into a distribution of masses and is a deconvolution problem rather than a chemical one. We return to the reagents and readouts that address these in Section 10, and would argue that progress will come from solving elution and deconvolution rather than from engineering another labeling enzyme.

What do these limitations mean for the body of work reviewed here? Applied to Table 3, they sort the published DDR proximity-labeling claims into two groups rather than casting doubt on all of them equally. Most of these studies used a single enzyme family, so their negative results are the weakest part of the record: a factor absent from a biotin-ligase neighborhood may be Lys-poor rather than absent, and no DDR study has yet reported the complementary-chemistry comparison that would settle it. Several of the scaffold and replisome maps used labeling windows of many hours, which makes them reliable inventories of steady-state neighborhoods but weak evidence for the order in which those neighborhoods assemble; damage-dependence inferred from such designs is a comparison of two averages, not a kinetic measurement. The peroxidase studies carry the opposite exposure: their temporal resolution is real, but the substrate pulse itself engages the response under study. And because several reports state neither the quantification mode, nor the replicate number, nor the scoring threshold, and two deposit no data at all, those datasets cannot be re-evaluated by a reader at all, not because they are wrong but because the information needed to judge them was not published. Read against this, a pattern emerges that we think is the most useful summary of the field's current evidential state: the PL-derived claims in the DDR that have survived are, almost without exception, those that were carried into an orthogonal assay. Shieldin was established by genetics rather than by the proximity map that nominated it; the stress-enhanced ZPR1 and ANP32A associations were confirmed by proximity ligation; RAD54L2 was validated by a sister-chromatid-exchange phenotype; the TRIP12–Ku70 association was confirmed in situ. The

proximity-labeling step in each case generated the hypothesis and did not, on its own, establish it. That is not a failure of the method but a statement of what it is for, and it sets the standard a new DDR proximity-labeling study should meet.

Table 3. Reported methodological parameters of the proximity-labeling studies in Table 2. Values are given only where the primary report states them; n.r., not reported or not located in the primary report. Accessions are given as deposited.

Study	Enzyme and Bait	Quantification	Key Specificity Control	Biological Replicates	Scoring	Threshold	Data Deposition	Proteins Reported
Gupta 2018 [19]	APEX2; 3 × FLAG–APEX2 knocked in at the N terminus of endogenous 53BP1, BRCA1, MDC1 (CRISPR–Cas9)	SILAC	Parental, non-engineered U2OS cells	6 per bait	MaxQuant/Andromeda	≥2-fold over control and quantified in ≥2 replicates; peptide and protein FDR < 0.01	PRIDE PXD009284	~400 bait-specific of >3500 identified
Chen 2025, preprint [18]	Phase-APEX2; split-APEX2 plus a light-controlled H_2O_2 generator (three-input AND gate)	n.r.	n.r.	n.r.	n.r.	n.r.	iProX IPX0013699000	n.r. (list defined by interaction density)
Jurkovic 2024 [20]	BioID2 fused to replisome subunits, ± hydroxyurea	LFQ (MaxQuant 1.6.17.0)	GFP–NLS	3	MaxQuant LFQ intensity ratio, bait (± HU) over untreated GFP–NLS	Protein present in ≥2 of 3 replicates	PRIDE PXD037136	654 proximal, 108 HU-responsive
Róna 2024 [21]; protocol [22]	TurboID; NLS–HA–TurboID–PCNA (and TurboID–cyclin D1)	Proteome Discoverer 1.4/SEQUEST	NLS–HA–TurboID (non-targeted enzyme), expression-matched by promoter choice	n.r.	n.r.	n.r.	MassIVE MSV000091006; PXD039228	n.r. (PSM fold changes reported graphically)
Zhu 2025 [23]	Chemically inducible split-APEX2 reconstituted by dual recognition of an R-loop and m^6A (m^6A-RLPL probe)	n.r. (streptavidin enrichment followed by HPLC–MS/MS)	Uninfected cells; no enzyme-only or no-probe arm reported for the proteomic experiment	3	n.r.	n.r.	None stated; data presented in the Supporting Information	1337 proximal, 71 differentially abundant
Wang 2025 [24]	APEX2; mitochondrially targeted G-quadruplex binder (MTS–SG4–APEX2)	n.r.	Binding-deficient mutant construct (mSG4–APEX2)	3	n.r.	n.r.	None; data stated to be available from the authors on request	206 candidate mtDNA G4-binding proteins
Schmidtmann 2016 [25]	BirA *–dCas9–eGFP (CasID)	Label-free	Same construct without sgRNA	4	Two-sided Student's *t*-test; protein required in ≥3 of 4 replicates	FDR 0.01, S0 0.1	n.r.	n.r. (volcano plots only)
Myers 2018 [26]	dCas9–APEX2 (CASPEX/GLoPro)	TMT, ratiometric	No-guide CASPEX cell line	4 sgRNA lines treated as replicates	Moderated one-sample *t*-test	n.r.	MassIVE PXD009187 (MSV000082154)	387 of 3199 enriched (telomere), 66 (c-MYC promoter)
Gao 2018 [27]	dCas9–APEX2 (C-BERST)	iBAQ/LFQ and three-state SILAC	Non-targeting sgRNA (sgNS); untransduced cells	2 (SILAC)	BH-adjusted *p* value	LFQ: BH $p < 0.05$ and log2 FC ≥ 2.0; SILAC: BH $p < 0.01$ and log2 FC ≥ 2.5	PRIDE PXD009216	359 enriched (telomere, LFQ), 460 of 1268 (centromere, SILAC)
Aprosoff 2023 [29]	BioID2–FLAG–SLX4 and SLX4–FLAG–BioID2, with parallel AP-MS	Spectral counts	BioID2–FLAG, BioID2–FLAG–eGFP and BioID2–FLAG–eGFP–NLS	3 per cell line	SAINTexpress 3.6.1	ProteinProphet ≥ 95% and ≥2 unique peptides	MassIVE MSV000090338; PXD036769	156 BioID2 and 81 AP-MS, 16 shared, 221 unique combined
Abbasi 2019 [30]	BioID (BirA *)–Ku70, with parallel AP-MS	Spectral counts	CRAPome v1.1 control set	n.r.	SAINTexpress via the CRAPome v1.1 interface	Protein and peptide FDR 1%	PRIDE PXD010930 and PXD010931	27 final, 22 shared between BioID and AP-MS
Abbasi 2023 [31]	Phospho-variant BioID2; Ku70 S155D and S155A	Label-free	S155A counterpart of the phospho-mimetic bait	3	SAINTexpress	FDR 1%, ≥1 unique peptide	PRIDE PXD025581	17 Ku70 S155D-specific of 193 candidates
Ho 2025 [32]	BioID (BirA *) on BLM, TOP3A, RMI1, RMI2; miniTurbo used separately for N- versus C-terminal BLM fusions	Spectral counts	n.r.	2 (BLM, TOP3A), 3 (RMI2), 6 (RMI1)	SAINTexpress	BFDR ≤ 0.01	MassIVE MSV000093876	206 high-confidence, 24 shared by two or more subunits

Abbreviations: LFQ, label-free quantification; SILAC, stable isotope labeling by amino acids in cell culture; TMT, tandem mass tags; iBAQ, intensity-based absolute quantification; BFDR, Bayesian false discovery rate; BH, Benjamini–Hochberg; n.r., not reported. Proteins reported gives the number of high-confidence proximal proteins stated by the primary study, with the total number identified where reported. Three studies state no thresholded count. Counts are not comparable across studies, which differ in bait, cell line, scoring model and threshold. BirA * denotes the promiscuous R118G mutant of bacterial BirA.

Across all of these issues, the consistent remedy is orthogonal validation: candidate interactions worth reporting should be confirmed by an independent method such as proximity ligation assay, co-immunoprecipitation, or imaging, and the most robust PL studies build this validation in rather than presenting the mass-spectrometry list as an endpoint.

9. Designing and Reporting a Nuclear Proximity-Labeling Experiment

The caveats above are actionable only if the workflow that produced a dataset is described in enough detail to be judged, and nuclear PL imposes requirements that work in

the cytoplasm does not. Chromatin-bound material must be released before capture, so lysis combines a strong denaturant with sonication or nuclease treatment, and the efficiency of that release sets which part of the labeled neighborhood is ever seen. Free biotin must be depleted before streptavidin capture, which is a particular concern for TurboID, which is active on endogenous biotin, so that its pulse begins before biotin is deliberately added and a biotin-free or dialyzed-serum period is the only true no-labeling control. Capture requires bead capacity in excess of the biotinylated load, and the stringency of the wash series, rather than the labeling chemistry, often decides the final list. Digestion is usually performed on bead, which leaves the biotinylated peptide bound to the resin and means that protein identifications derive from the unmodified peptides of a labeled protein.

That last point has a corollary that bears on every caveat in Section 8: a protein identified after streptavidin enrichment is not necessarily a protein that was labeled. Unmodified proteins that remain bound to a biotinylated partner through the washes are recovered alongside genuinely labeled ones, and bottom-up identification cannot separate the two. Enrichment of biotinylated peptides with anti-biotin antibodies resolves this directly [39], and the same site-level data would answer the residue- and modification-bias questions raised above, which at present are argued from chemistry rather than measured.

Quantitative design decides what a fold change means. A bait fusion and a non-targeted enzyme biotinylate with different total efficiency, so the comparison between them rests on normalization rather than subtraction: an analysis should state what was held constant, whether total captured protein, bait expression, an isotopic spike-in or median-centered log ratios, and at which step the conditions were combined. The choice of anchor decides what a fold change means, so it should be named rather than left implicit. The labeling scheme is not neutral here. Metabolic labeling allows conditions to be mixed before capture, so variation in enrichment is internally controlled; isobaric labeling requires separate captures that are pooled afterwards, so enrichment variability is not internally controlled by default, although an internal reference channel, carrier or bridge designs and appropriate normalization can mitigate this substantially, which makes the limitation a property of the design rather than of the chemistry. Ratio compression is a separate matter. It arises from co-isolation of near-isobaric precursors and therefore depends on the acquisition and quantification strategy, including isolation window width, the exclusion of chimeric spectra and the use of MS3 or real-time-search approaches, rather than being an inherent consequence of isobaric tagging. Label-free comparison avoids both concerns but is the most exposed to missing values. With missing values the pattern matters more than the count, since a value missing because the protein is genuinely absent from the control is informative whereas a value missing at random is not, and the imputation strategy has to be reported because it determines the fold changes at the top of the ranked list, which is where candidates are selected. A hazard specific to PL is that labeling efficiency is itself treatment-dependent: biotin ligases consume ATP, and an insult that hyperactivates PARP depletes NAD^+ and ATP (Section 8), so an apparent damage-dependent loss of proximal proteins may be metabolic rather than compositional. A streptavidin blot or equivalent loading readout for every condition should accompany any differential experiment.

Two further points are routinely omitted. Acquisition mode matters more in PL than in most applications, because streptavidin eluates are low-input and the informative experiments compare many conditions at once, which is exactly the regime in which data-dependent acquisition (DDA) loses the weak, transient partners the method exists to capture, because its selection of precursors is stochastic. Data-independent acquisition (DIA) [101] is the better match for the multi-condition designs proposed in Sections 4 and 8. DIA acquires fragment spectra for all precursors within defined windows, which removes run-to-run selection variability and reduces missing values across a multi-condition series, at the cost

of more demanding spectral deconvolution and the need for either a project-specific library or a library-free search. DIA is almost absent from the DDR proximity-labeling literature so far, as Table 3 shows, which makes it an open opportunity rather than a settled preference. Identification is also reported at the level of protein groups, which in this field is not a formality, shared peptides make several of the most relevant species hard to resolve, histone variants among them, so the group-level false-discovery treatment and the handling of single-peptide identifications belong in the methods rather than in a Supplementary File. Table 3 compiles these parameters for the studies in Table 2, and the gaps in it are themselves informative: several reports do not state the quantification mode, the number of biological replicates or the scoring threshold, and two deposit no data at all. Raw files and search outputs should be deposited in a public proteomics repository [102] with the search parameters stated, including the biotin and biotin-phenol adducts as variable modifications. A dataset whose enrichment chemistry, normalization, acquisition mode, scoring model and deposition are all stated can be re-evaluated by a reader; one that reports only a list of gene names cannot.

10. Future Perspectives

Three methodological directions are likely to shape the field, with a fourth, more applied one emerging alongside them. Spatiotemporal resolution will improve as photocatalytic and split systems with shorter, tunable radii mature, allowing labeling to be confined to a specific lesion, condensate, or subcompartment and triggered with light at a chosen moment after damage. Combinatorial logic, meaning split enzymes reconstituted only at defined protein–protein or protein–structure coincidences and AND-gate designs that require several inputs at once, will shift PL from cataloging neighborhoods toward testing specific hypotheses about where and with what a factor associates. And integration will deepen: pairing PL with nascent-DNA capture, cross-linking mass spectrometry, structural prediction, network analysis, and RNA-side proximity labeling, which assigns transcripts rather than proteins to a subcellular neighborhood [103] and is the obvious route to the damage-induced non-coding RNAs that seed repair compartments, will let spatial interactomes be read not as isolated lists but as mechanistic models. Integration with modification-resolved and top-down workflows is the natural complement to the proteoform routes set out in Section 8. That such readouts are becoming feasible on chromatin substrates is clear from intact-protein sequencing that localizes co-occurring histone modifications directly, up to seven acetylation sites on a single histone H4 molecule, instead of inferring them from separate peptides [104]. The reagent that would make the coupling practical already exists: desthiobiotin probes bind streptavidin reversibly and elute under mild conditions [105], though they have not yet been paired with an intact-protein readout of a proximity-labeling experiment. That pairing, rather than another labeling enzyme, is the experiment we would most like to see attempted. A further, more applied direction is the move out of cell lines: TurboID already functions in whole organisms and tissues [35], and applying damage-responsive proximity labeling in tumors, comparing the repair neighborhoods of drug-sensitive and drug-resistant disease or of normal and transformed tissue, would connect spatial DDR interactomics directly to therapeutic resistance, where the routes to resistance, which include restored BRCA function, fork stabilization and altered chromatin remodeling [106], remain only partly resolved [107,108]. The trajectory of the last few years, from PL as one proteomics accessory among many to PL as a primary route to new DDR biology, suggests that the limiting factor going forward will be the sharpness of the biological question and the rigor of validation, more than any further advance in enzymes.

Author Contributions: Conceptualization, G.S. and W.K.; writing—original draft preparation, J.A., S.Q. and W.K.; writing—review and editing, S.Q., S.T., Z.X., G.S. and W.K.; supervision, G.S. and W.K.; project administration, G.S. and W.K.; funding acquisition, W.K. All authors have read and agreed to the published version of the manuscript.

Funding: This research was supported by the National Research Foundation of Korea (NRF) grants (2022R1A2C1091563, RS-2025-02293074), the Global-Learning & Academic Research Institution for Master's PhD students and Postdocs (G-LAMP) Program of the NRF funded by the Ministry of Education (RS-2025-25441283). The following are results of a study on the "Glocal University Project," supported by the Ministry of Education of Korea, Chungnam RISE, and Soonchunhyang University.

Institutional Review Board Statement: Not applicable.

Informed Consent Statement: Not applicable.

Data Availability Statement: No new data were created or analyzed in this study. Data sharing is not applicable to this article.

Acknowledgments: The authors declare that no generative artificial intelligence or large-language model tools were employed for drafting, data analysis or figure generation in this work.

Conflicts of Interest: The authors declare no conflicts of interest.

References

1. Rogakou, E.P.; Boon, C.; Redon, C.; Bonner, W.M. Megabase chromatin domains involved in DNA double-strand breaks in vivo. *J. Cell Biol.* **1999**, *146*, 905–916. [CrossRef] [PubMed]
2. Burma, S.; Chen, B.P.; Murphy, M.; Kurimasa, A.; Chen, D.J. ATM phosphorylates histone H2AX in response to DNA double-strand breaks. *J. Biol. Chem.* **2001**, *276*, 42462–42467. [CrossRef] [PubMed]
3. Stewart, G.S.; Wang, B.; Bignell, C.R.; Taylor, A.M.R.; Elledge, S.J. MDC1 is a mediator of the mammalian DNA damage checkpoint. *Nature* **2003**, *421*, 961–966. [CrossRef]
4. Bekker-Jensen, S.; Mailand, N. The ubiquitin- and SUMO-dependent signaling response to DNA double-strand breaks. *FEBS Lett.* **2011**, *585*, 2914–2919. [CrossRef] [PubMed]
5. Wilson, M.D.; Benlekbir, S.; Fradet-Turcotte, A.; Sherker, A.; Julien, J.-P.; McEwan, A.; Noordermeer, S.M.; Sicheri, F.; Rubinstein, J.L.; Durocher, D. The structural basis of modified nucleosome recognition by 53BP1. *Nature* **2016**, *536*, 100–103. [CrossRef] [PubMed]
6. Tarsounas, M.; Sung, P. The antitumorigenic roles of BRCA1-BARD1 in DNA repair and replication. *Nat. Rev. Mol. Cell Biol.* **2020**, *21*, 284–299. [CrossRef] [PubMed]
7. Nakamura, K.; Saredi, G.; Becker, J.R.; Foster, B.M.; Nguyen, N.V.; Beyer, T.E.; Cesa, L.C.; Faull, P.A.; Lukauskas, S.; Frimurer, T.; et al. H4K20me0 recognition by BRCA1-BARD1 directs homologous recombination to sister chromatids. *Nat. Cell Biol.* **2019**, *21*, 311–318. [CrossRef] [PubMed]
8. Zhao, F.; Kim, W.; Kloeber, J.A.; Lou, Z. DNA end resection and its role in DNA replication and DSB repair choice in mammalian cells. *Exp. Mol. Med.* **2020**, *52*, 1705–1714. [CrossRef]
9. Zimmermann, M.; de Lange, T. 53BP1: Pro choice in DNA repair. *Trends Cell Biol.* **2014**, *24*, 108–117. [CrossRef] [PubMed]
10. He, L.; Moon, J.; Cai, C.; Hao, Y.; Lee, H.; Kim, W.; Zhao, F.; Lou, Z. The interplay between chromatin remodeling and DNA double-strand break repair: Implications for cancer biology and therapeutics. *DNA Repair* **2025**, *146*, 103811. [CrossRef] [PubMed]
11. Matsuoka, S.; Ballif, B.A.; Smogorzewska, A.; McDonald, E.R., III; Hurov, K.E.; Luo, J.; Bakalarski, C.E.; Zhao, Z.; Solimini, N.; Lerenthal, Y.; et al. ATM and ATR substrate analysis reveals extensive protein networks responsive to DNA damage. *Science* **2007**, *316*, 1160–1166. [CrossRef] [PubMed]
12. Zeng, M.; Tang, Z.; Li, C.; Ren, L.; Wang, X.; Carr, A.; Liu, C. CDW19S coordinates phasic end processing via distinct enzymatic activities. *Nucleic Acids Res.* **2026**, *54*, gkag681. [CrossRef] [PubMed]
13. Qin, W.; Cho, K.F.; Cavanagh, P.E.; Ting, A.Y. Deciphering molecular interactions by proximity labeling. *Nat. Methods* **2021**, *18*, 133–143. [CrossRef]
14. van Steensel, B.; Henikoff, S. Identification of in vivo DNA targets of chromatin proteins using tethered Dam methyltransferase. *Nat. Biotechnol.* **2000**, *18*, 424–428. [CrossRef] [PubMed]
15. Ummethum, H.; Hamperl, S. Proximity labeling techniques to study chromatin. *Front. Genet.* **2020**, *11*, 450. [CrossRef] [PubMed]
16. Tong, F.; Seath, C.P. Proximity labeling tools for studying chromatin interactomes. *Curr. Opin. Chem. Biol.* **2026**, *93*, 102686. [CrossRef] [PubMed]

17. Muralidharan, M.; Krogan, N.J.; Bouhaddou, M.; Kim, M. Current proteomics methods applicable to dissecting the DNA damage response. *NAR Cancer* **2023**, *5*, zcad020. [CrossRef] [PubMed]
18. Chen, Z.; Chen, Y.; Ding, H.; Huang, M.; Chen, W.; Fu, B.; Wang, M.; Zhang, L.; Qin, W.; Li, P. Mapping core components of membrane-less organelles in living cells by Phase-APEX2 proximity labeling. *bioRxiv* **2025**. *preprint*. [CrossRef]
19. Gupta, R.; Somyajit, K.; Narita, T.; Maskey, E.; Stanlie, A.; Kremer, M.; Typas, D.; Lammers, M.; Mailand, N.; Nussenzweig, A.; et al. DNA repair network analysis reveals shieldin as a key regulator of NHEJ and PARP inhibitor sensitivity. *Cell* **2018**, *173*, 972–988.e23. [CrossRef]
20. Jurkovic, C.-M.; Raisch, J.; Tran, S.; Nguyen, H.D.; Lévesque, D.; Scott, M.S.; Campos, E.I.; Boisvert, F.-M. Replisome proximal protein associations and dynamic proteomic changes at stalled replication forks. *Mol. Cell. Proteom.* **2024**, *23*, 100767. [CrossRef] [PubMed]
21. Rona, G.; Miwatani-Minter, B.; Zhang, Q.; Goldberg, H.V.; Kerzhnerman, M.A.; Howard, J.B.; Simoneschi, D.; Lane, E.; Hobbs, J.W.; Sassani, E.; et al. CDK-independent role of D-type cyclins in regulating DNA mismatch repair. *Mol. Cell* **2024**, *84*, 1224–1242.e13. [CrossRef]
22. Borosta, R.; Szepesi-Nagy, I.; Kató, I.; Róna, G. Protocol for identifying DNA damage responders through proximity biotinylation of proliferating cell nuclear antigen interactors. *STAR Protoc.* **2025**, *6*, 104136. [CrossRef] [PubMed]
23. Zhu, M.-D.; Yin, H.-Q.; He, Z.-D.; Cheng, Y.; Ye, Q.-Q.; Wang, Z.-G.; Pang, D.-W.; Liu, S.-L. Spatial mapping and interactome profiling of m^{6}A-modified R-loops via chemically inducible split-APEX2 proximity labeling. *Anal. Chem.* **2025**, *97*, 27364–27374. [CrossRef] [PubMed]
24. Wang, X.; Qin, G.; Yang, J.; Zhao, C.; Ren, J.; Qu, X. A subcellular selective APEX2-based proximity labeling used for identifying mitochondrial G-quadruplex DNA binding proteins. *Nucleic Acids Res.* **2025**, *53*, gkae1259. [CrossRef]
25. Schmidtmann, E.; Anton, T.; Rombaut, P.; Herzog, F.; Leonhardt, H. Determination of local chromatin composition by CasID. *Nucleus* **2016**, *7*, 476–484. [CrossRef] [PubMed]
26. Myers, S.A.; Wright, J.; Peckner, R.; Kalish, B.T.; Zhang, F.; Carr, S.A. Discovery of proteins associated with a predefined genomic locus via dCas9–APEX-mediated proximity labeling. *Nat. Methods* **2018**, *15*, 437–439. [CrossRef]
27. Gao, X.D.; Tu, L.-C.; Mir, A.; Rodriguez, T.; Ding, Y.; Leszyk, J.; Dekker, J.; Shaffer, S.A.; Zhu, L.J.; Wolfe, S.A.; et al. C-BERST: Defining subnuclear proteomic landscapes at genomic elements with dCas9-APEX2. *Nat. Methods* **2018**, *15*, 433–436. [CrossRef] [PubMed]
28. Doi, G.; Okada, S.; Yasukawa, T.; Sugiyama, Y.; Bala, S.; Miyazaki, S.; Kang, D.; Ito, T. Catalytically inactive Cas9 impairs DNA replication fork progression to induce focal genomic instability. *Nucleic Acids Res.* **2021**, *49*, 954–968. [CrossRef] [PubMed]
29. Aprosoff, C.M.; Dyakov, B.J.A.; Cheung, V.H.W.; Wong, C.J.; Palandra, M.; Gingras, A.-C.; Wyatt, H.D.M. Comprehensive interactome mapping of the DNA repair scaffold SLX4 using proximity labeling and affinity purification. *J. Proteome Res.* **2023**, *22*, 1660–1681. [CrossRef] [PubMed]
30. Abbasi, S.; Schild-Poulter, C. Mapping the Ku interactome using proximity-dependent biotin identification in human cells. *J. Proteome Res.* **2019**, *18*, 1064–1077. [CrossRef] [PubMed]
31. Abbasi, S.; Bayat, L.; Schild-Poulter, C. Analysis of Ku70 S155 phospho-specific BioID2 interactome identifies Ku association with TRIP12 in response to DNA damage. *Int. J. Mol. Sci.* **2023**, *24*, 7041. [CrossRef] [PubMed]
32. Ho, J.J.; Cheng, E.; Wong, C.J.; St-Germain, J.R.; Dunham, W.H.; Raught, B.; Gingras, A.C.; Brown, G.W. The BLM-TOP3A-RMI1-RMI2 proximity map reveals that RAD54L2 suppresses sister chromatid exchanges. *EMBO Rep.* **2025**, *26*, 1290–1314. [CrossRef] [PubMed]
33. Roux, K.J.; Kim, D.I.; Raida, M.; Burke, B. A promiscuous biotin ligase fusion protein identifies proximal and interacting proteins in mammalian cells. *J. Cell Biol.* **2012**, *196*, 801–810. [CrossRef] [PubMed]
34. Kim, D.I.; Jensen, S.C.; Noble, K.A.; KC, B.; Roux, K.H.; Motamedchaboki, K.; Roux, K.J. An improved smaller biotin ligase for BioID proximity labeling. *Mol. Biol. Cell* **2016**, *27*, 1188–1196. [CrossRef] [PubMed]
35. Branon, T.C.; Bosch, J.A.; Sanchez, A.D.; Udeshi, N.D.; Svinkina, T.; Carr, S.A.; Feldman, J.L.; Perrimon, N.; Ting, A.Y. Efficient proximity labeling in living cells and organisms with TurboID. *Nat. Biotechnol.* **2018**, *36*, 880–887, Correction in *Nat. Biotechnol.* **2020**, *38*, 108. [CrossRef] [PubMed]
36. Kubitz, L.; Bitsch, S.; Zhao, X.; Schmitt, K.; Deweid, L.; Roehrig, A.; Barazzone, E.C.; Valerius, O.; Kolmar, H.; Béthune, J. Engineering of ultraID, a compact and hyperactive enzyme for proximity-dependent biotinylation in living cells. *Commun. Biol.* **2022**, *5*, 657. [CrossRef] [PubMed]
37. Rhee, H.-W.; Zou, P.; Udeshi, N.D.; Martell, J.D.; Mootha, V.K.; Carr, S.A.; Ting, A.Y. Proteomic mapping of mitochondria in living cells via spatially restricted enzymatic tagging. *Science* **2013**, *339*, 1328–1331. [CrossRef] [PubMed]
38. Lam, S.S.; Martell, J.D.; Kamer, K.J.; Deerinck, T.J.; Ellisman, M.H.; Mootha, V.K.; Ting, A.Y. Directed evolution of APEX2 for electron microscopy and proximity labeling. *Nat. Methods* **2015**, *12*, 51–54. [CrossRef] [PubMed]

39. Udeshi, N.D.; Pedram, K.; Svinkina, T.; Fereshetian, S.; Myers, S.A.; Aygun, O.; Krug, K.; Clauser, K.; Ryan, D.; Ast, T.; et al. Antibodies to biotin enable large-scale detection of biotinylation sites on proteins. *Nat. Methods* **2017**, *14*, 1167–1170. [CrossRef] [PubMed]
40. Battison, A.S.; Balsbaugh, J.L.; Borniger, J.C. APEX2 and TurboID define unique subcellular proteomes. *Sci. Rep.* **2025**, *15*, 43547. [CrossRef] [PubMed]
41. Schopp, I.M.; Amaya Ramirez, C.C.; Debeljak, J.; Kreibich, E.; Skribbe, M.; Wild, K.; Béthune, J. Split-BioID a conditional proteomics approach to monitor the composition of spatiotemporally defined protein complexes. *Nat. Commun.* **2017**, *8*, 15690. [CrossRef] [PubMed]
42. Cho, K.F.; Branon, T.C.; Rajeev, S.; Svinkina, T.; Udeshi, N.D.; Thoudam, T.; Kwak, C.; Rhee, H.W.; Lee, I.K.; Carr, S.A.; et al. Split-TurboID enables contact-dependent proximity labeling in cells. *Proc. Natl. Acad. Sci. USA* **2020**, *117*, 12143–12154. [CrossRef] [PubMed]
43. Han, Y.; Branon, T.C.; Martell, J.D.; Boassa, D.; Shechner, D.; Ellisman, M.H.; Ting, A. Directed evolution of split APEX2 peroxidase. *ACS Chem. Biol.* **2019**, *14*, 619–635, Correction in *ACS Chem. Biol.* **2019**, *14*, 2942. [CrossRef] [PubMed]
44. Knutson, S.D.; Buksh, B.F.; Huth, S.W.; Morgan, D.C.; MacMillan, D.W.C. Current advances in photocatalytic proximity labeling. *Cell Chem. Biol.* **2024**, *31*, 1145–1161. [CrossRef] [PubMed]
45. Geri, J.B.; Oakley, J.V.; Reyes-Robles, T.; Wang, T.; McCarver, S.J.; White, C.H.; Rodriguez-Rivera, F.P.; Parker, D.L.; Hett, E.C.; Fadeyi, O.O.; et al. Microenvironment mapping via Dexter energy transfer on immune cells. *Science* **2020**, *367*, 1091–1097. [CrossRef] [PubMed]
46. Seath, C.P.; Burton, A.J.; Sun, X.; Lee, G.; Kleiner, R.E.; MacMillan, D.W.C.; Muir, T.W. Tracking chromatin state changes using nanoscale photo-proximity labelling. *Nature* **2023**, *616*, 574–580. [CrossRef] [PubMed]
47. Trifault, B.; Mamontova, V.; Burger, K. In vivo proximity labeling of nuclear and nucleolar proteins by a stably expressed, DNA damage-responsive NONO-APEX2 fusion protein. *Front. Mol. Biosci.* **2022**, *9*, 914873. [CrossRef] [PubMed]
48. Yang, Z.; Zhang, Y.; Fang, Y.; Zhang, Y.; Du, J.; Shen, X.; Zhang, K.; Zou, P.; Chen, Z. Spatial barcoding reveals reaction radii and contact-dependent mechanism of proximity labeling. *Nat. Chem. Biol.* **2025**. [CrossRef] [PubMed]
49. Noordermeer, S.M.; Adam, S.; Setiaputra, D.; Barazas, M.; Pettitt, S.J.; Ling, A.K.; Olivieri, M.; Álvarez-Quilón, A.; Moatti, N.; Zimmermann, M.; et al. The shieldin complex mediates 53BP1-dependent DNA repair. *Nature* **2018**, *560*, 117–121. [CrossRef] [PubMed]
50. Dev, H.; Chiang, T.-W.W.; Lescale, C.; de Krijger, I.; Martin, A.G.; Pilger, D.; Coates, J.; Sczaniecka-Clift, M.; Wei, W.; Ostermaier, M.; et al. Shieldin complex promotes DNA end-joining and counters homologous recombination in BRCA1-null cells. *Nat. Cell Biol.* **2018**, *20*, 954–965. [CrossRef] [PubMed]
51. Ghezraoui, H.; Oliveira, C.; Becker, J.R.; Bilham, K.; Moralli, D.; Anzilotti, C.; Fischer, R.; Deobagkar-Lele, M.; Sanchiz-Calvo, M.; Fueyo-Marcos, E.; et al. 53BP1 cooperation with the REV7-shieldin complex underpins DNA structure-specific NHEJ. *Nature* **2018**, *560*, 122–127. [CrossRef] [PubMed]
52. Boersma, V.; Moatti, N.; Segura-Bayona, S.; Peuscher, M.H.; van der Torre, J.; Wevers, B.A.; Orthwein, A.; Durocher, D.; Jacobs, J.J.L. MAD2L2 controls DNA repair at telomeres and DNA breaks by inhibiting 5′ end resection. *Nature* **2015**, *521*, 537–540. [CrossRef] [PubMed]
53. Chapman, J.R.; Barral, P.; Vannier, J.-B.; Borel, V.; Steger, M.; Tomas-Loba, A.; Sartori, A.A.; Adams, I.R.; Batista, F.D.; Boulton, S.J. RIF1 is essential for 53BP1-dependent nonhomologous end joining and suppression of DNA double-strand break resection. *Mol. Cell* **2013**, *49*, 858–871, Erratum in *Mol. Cell* **2021**, *81*, 2868. [CrossRef] [PubMed]
54. Banani, S.F.; Lee, H.O.; Hyman, A.A.; Rosen, M.K. Biomolecular condensates: Organizers of cellular biochemistry. *Nat. Rev. Mol. Cell Biol.* **2017**, *18*, 285–298. [CrossRef] [PubMed]
55. Kilic, S.; Lezaja, A.; Gatti, M.; Bianco, E.; Michelena, J.; Imhof, R.; Altmeyer, M. Phase separation of 53BP1 determines liquid-like behavior of DNA repair compartments. *EMBO J.* **2019**, *38*, e101379. [CrossRef] [PubMed]
56. Ochs, F.; Karemore, G.; Miron, E.; Brown, J.; Sedlackova, H.; Rask, M.-B.; Lampe, M.; Buckle, V.; Schermelleh, L.; Lukas, J.; et al. Stabilization of chromatin topology safeguards genome integrity. *Nature* **2019**, *574*, 571–574. [CrossRef] [PubMed]
57. Pessina, F.; Giavazzi, F.; Yin, Y.; Gioia, U.; Vitelli, V.; Galbiati, A.; Barozzi, S.; Garre, M.; Oldani, A.; Flaus, A.; et al. Functional transcription promoters at DNA double-strand breaks mediate RNA-driven phase separation of damage-response factors. *Nat. Cell Biol.* **2019**, *21*, 1286–1299. [CrossRef] [PubMed]
58. Li, L.; Yao, L.; Wang, M.; Zhou, X.; Xu, Y. Phase separation in DNA damage response: New insights into cancer development and therapy. *Biochim. Biophys. Acta Rev. Cancer* **2024**, *1879*, 189206. [CrossRef] [PubMed]
59. Wang, Y.-L.; Zhao, W.-W.; Bai, S.-M.; Feng, L.-L.; Bie, S.-Y.; Gong, L.; Wang, F.; Wei, M.-B.; Feng, W.-X.; Pang, X.-L.; et al. MRNIP condensates promote DNA double-strand break sensing and end resection. *Nat. Commun.* **2022**, *13*, 2638. [CrossRef] [PubMed]
60. Altmeyer, M.; Neelsen, K.J.; Teloni, F.; Pozdnyakova, I.; Pellegrino, S.; Grøfte, M.; Rask, M.-B.D.; Streicher, W.; Jungmichel, S.; Nielsen, M.L.; et al. Liquid demixing of intrinsically disordered proteins is seeded by poly(ADP-ribose). *Nat. Commun.* **2015**, *6*, 8088. [CrossRef] [PubMed]

61. Singatulina, A.S.; Hamon, L.; Sukhanova, M.V.; Desforges, B.; Joshi, V.; Bouhss, A.; Lavrik, O.I.; Pastré, D. PARP-1 activation directs FUS to DNA damage sites to form PARG-reversible compartments enriched in damaged DNA. *Cell Rep.* **2019**, *27*, 1809–1821.e5. [CrossRef] [PubMed]
62. Song, S.; Xie, H.; Wang, Q.; Sun, X.; Xu, J.; Chen, R.; Zhu, Y.; Jiang, L.; Ding, X. Spatiotemporal deciphering of dynamic the FUS interactome during liquid–liquid phase separation in living cells. *Nat. Commun.* **2025**, *16*, 4328. [CrossRef] [PubMed]
63. Sirbu, B.M.; Couch, F.B.; Feigerle, J.T.; Bhaskara, S.; Hiebert, S.W.; Cortez, D. Analysis of protein dynamics at active, stalled, and collapsed replication forks. *Genes Dev.* **2011**, *25*, 1320–1327. [CrossRef] [PubMed]
64. Adolph, M.B.; Cortez, D. Mechanisms and regulation of replication fork reversal. *DNA Repair* **2024**, *141*, 103731. [CrossRef] [PubMed]
65. Dungrawala, H.; Rose, K.L.; Bhat, K.P.; Mohni, K.N.; Glick, G.G.; Couch, F.B.; Cortez, D. The replication checkpoint prevents two types of fork collapse without regulating replisome stability. *Mol. Cell* **2015**, *59*, 998–1010. [CrossRef] [PubMed]
66. Belotserkovskii, B.P.; Tornaletti, S.; D'Souza, A.D.; Hanawalt, P.C. R-loop generation during transcription: Formation, processing and cellular outcomes. *DNA Repair* **2018**, *71*, 69–81. [CrossRef] [PubMed]
67. Silva, S.; Guillén-Mendoza, C.; Aguilera, A. RNase H1 hybrid-binding domain-based tools for cellular biology studies of DNA-RNA hybrids in mammalian cells. In *R-Loops*; Methods in Molecular Biology; Humana Press: New York, NY, USA, 2022; Volume 2528, pp. 115–125. [CrossRef] [PubMed]
68. Qiu, Y.; Man, C.; Zhu, L.; Zhang, S.; Wang, X.; Gong, D.; Fan, Y. R-loops' m^6A modification and its roles in cancers. *Mol. Cancer* **2024**, *23*, 232. [CrossRef]
69. Larsen, N.B.; Gao, A.O.; Sparks, J.L.; Gallina, I.; Wu, R.A.; Mann, M.; Räschle, M.; Walter, J.C.; Duxin, J.P. Replication-coupled DNA-protein crosslink repair by SPRTN and the proteasome in Xenopus egg extracts. *Mol. Cell* **2019**, *73*, 574–588.e7. [CrossRef] [PubMed]
70. Wojtaszek, J.L.; Williams, R.S. From the TOP: Formation, recognition and resolution of topoisomerase DNA protein crosslinks. *DNA Repair* **2024**, *142*, 103751. [CrossRef] [PubMed]
71. Perry, M.; Ghosal, G. Mechanisms and regulation of DNA-protein crosslink repair during DNA replication by SPRTN protease. *Front. Mol. Biosci.* **2022**, *9*, 916697. [CrossRef] [PubMed]
72. Sun, Y.; Saha, L.K.; Saha, S.; Jo, U.; Pommier, Y. Debulking of topoisomerase DNA-protein crosslinks (TOP-DPC) by the proteasome, non-proteasomal and non-proteolytic pathways. *DNA Repair* **2020**, *94*, 102926. [CrossRef] [PubMed]
73. Kojima, Y.; Machida, Y.; Palani, S.; Caulfield, T.R.; Radisky, E.S.; Kaufmann, S.H.; Machida, Y.J. FAM111A protects replication forks from protein obstacles via its trypsin-like domain. *Nat. Commun.* **2020**, *11*, 1318. [CrossRef] [PubMed]
74. Serbyn, N.; Noireterre, A.; Bagdiul, I.; Plank, M.; Michel, A.H.; Loewith, R.; Kornmann, B.; Stutz, F. The aspartic protease Ddi1 contributes to DNA-protein crosslink repair in yeast. *Mol. Cell* **2020**, *77*, 1066–1079.e9. [CrossRef] [PubMed]
75. Borgermann, N.; Ackermann, L.; Schwertman, P.; Hendriks, I.A.; Thijssen, K.; Liu, J.C.; Lans, H.; Nielsen, M.L.; Mailand, N. SUMOylation promotes protective responses to DNA-protein crosslinks. *EMBO J.* **2019**, *38*, e101496. [CrossRef] [PubMed]
76. Fábián, Z.; Kakulidis, E.S.; Hendriks, I.A.; Kühbacher, U.; Larsen, N.B.; Oliva-Santiago, M.; Wang, J.; Leng, X.; Dirac-Svejstrup, A.B.; Svejstrup, J.Q.; et al. PARP1-dependent DNA-protein crosslink repair. *Nat. Commun.* **2024**, *15*, 6641. [CrossRef] [PubMed]
77. Krastev, D.B.; Li, S.; Sun, Y.; Wicks, A.J.; Hoslett, G.; Weekes, D.; Badder, L.M.; Knight, E.G.; Marlow, R.; Pardo, M.C.; et al. The ubiquitin-dependent ATPase p97 removes cytotoxic trapped PARP1 from chromatin. *Nat. Cell Biol.* **2022**, *24*, 62–73. [CrossRef] [PubMed]
78. Carnie, C.J.; Acampora, A.C.; Bader, A.S.; Erdenebat, C.; Zhao, S.; Bitensky, E.; van den Heuvel, D.; Parnas, A.; Gupta, V.; D'Alessandro, G.; et al. Transcription-coupled repair of DNA–protein cross-links depends on CSA and CSB. *Nat. Cell Biol.* **2024**, *26*, 797–810. [CrossRef] [PubMed]
79. Bhattacharjee, S.; Rehman, I.; Nandy, S.; Das, B.B. Post-translational regulation of tyrosyl-DNA phosphodiesterase (TDP1 and TDP2) for the repair of the trapped topoisomerase-DNA covalent complex. *DNA Repair* **2022**, *111*, 103277. [CrossRef] [PubMed]
80. Schellenberg, M.J.; Lieberman, J.A.; Herrero-Ruiz, A.; Butler, L.R.; Williams, J.G.; Muñoz-Cabello, A.M.; Mueller, G.A.; London, R.E.; Cortés-Ledesma, F.; Williams, R.S. ZATT (ZNF451)-mediated resolution of topoisomerase 2 DNA-protein cross-links. *Science* **2017**, *357*, 1412–1416. [CrossRef] [PubMed]
81. Lascaux, P.; Hoslett, G.; Tribble, S.; Trugenberger, C.; Antičević, I.; Otten, C.; Torrecilla, I.; Koukouravas, S.; Zhao, Y.; Yang, H.; et al. TEX264 drives selective autophagy of DNA lesions to promote DNA repair and cell survival. *Cell* **2024**, *187*, 5698–5718.e26. [CrossRef] [PubMed]
82. Räschle, M.; Smeenk, G.; Hansen, R.K.; Temu, T.; Oka, Y.; Hein, M.Y.; Nagaraj, N.; Long, D.T.; Walter, J.C.; Hofmann, K.; et al. Proteomics reveals dynamic assembly of repair complexes during bypass of DNA cross-links. *Science* **2015**, *348*, 1253671. [CrossRef] [PubMed]
83. Déjardin, J.; Kingston, R.E. Purification of proteins associated with specific genomic loci. *Cell* **2009**, *136*, 175–186. [CrossRef] [PubMed]

84. Ugur, E.; Bartoschek, M.D.; Leonhardt, H. Locus-specific chromatin proteome revealed by mass spectrometry-based CasID. In *The Nucleus*; Methods in Molecular Biology; Humana Press: New York, NY, USA, 2020; Volume 2175, pp. 109–121. [CrossRef] [PubMed]
85. Zhou, J.; Li, X.; Wen, Q.; Gan, H. Antibody-mediated protein A–APEX2 labeling (AMAPEX) for proximity proteome exploration. In *Proximity-Dependent Protein Biotinylation*; Methods in Molecular Biology; Humana Press: New York, NY, USA, 2025; Volume 2953, pp. 295–310. [CrossRef] [PubMed]
86. Villaseñor, R.; Pfaendler, R.; Ambrosi, C.; Butz, S.; Giuliani, S.; Bryan, E.; Sheahan, T.W.; Gable, A.L.; Schmolka, N.; Manzo, M.; et al. ChromID identifies the protein interactome at chromatin marks. *Nat. Biotechnol.* **2020**, *38*, 728–736, Correction in *Nat. Biotechnol.* **2020**, *38*, 757. [CrossRef] [PubMed]
87. Iacovoni, J.S.; Caron, P.; Lassadi, I.; Nicolas, E.; Massip, L.; Trouche, D.; Legube, G. High-resolution profiling of γH2AX around DNA double strand breaks in the mammalian genome. *EMBO J.* **2010**, *29*, 1446–1457. [CrossRef] [PubMed]
88. Laughery, M.F.; Mayes, H.C.; Pedroza, I.K.; Wyrick, J.J. R-loop formation by dCas9 is mutagenic in *Saccharomyces cerevisiae*. *Nucleic Acids Res.* **2019**, *47*, 2389–2401. [CrossRef] [PubMed]
89. Kim, D.I.; Birendra, K.C.; Zhu, W.; Motamedchaboki, K.; Doye, V.; Roux, K.J. Probing nuclear pore complex architecture with proximity-dependent biotinylation. *Proc. Natl. Acad. Sci. USA* **2014**, *111*, E2453–E2461. [CrossRef] [PubMed]
90. Douglas, C.J.; Samowitz, P.; Tong, F.; Long, A.; Bradley, C.M.; Radnai, L.; MacMillan, D.W.C.; Miller, C.A.; Rumbaugh, G.; Seath, C.P. Mesoscale proximity labeling at chromatin leads to identification of small molecule mechanism of action. *Nat. Commun.* **2026**, *17*, 10123. [CrossRef] [PubMed]
91. Barzilai, A.; Yamamoto, K.-I. DNA damage responses to oxidative stress. *DNA Repair* **2004**, *3*, 1109–1115. [CrossRef] [PubMed]
92. Schraufstatter, I.U.; Hinshaw, D.B.; Hyslop, P.A.; Spragg, R.G.; Cochrane, C.G. Oxidant injury of cells. DNA strand-breaks activate polyadenosine diphosphate-ribose polymerase and lead to depletion of nicotinamide adenine dinucleotide. *J. Clin. Investig.* **1986**, *77*, 1312–1320. [CrossRef] [PubMed]
93. Hung, V.; Udeshi, N.D.; Lam, S.S.; Loh, K.H.; Cox, K.J.; Pedram, K.; Carr, S.A.; Ting, A.Y. Spatially resolved proteomic mapping in living cells with the engineered peroxidase APEX2. *Nat. Protoc.* **2016**, *11*, 456–475. [CrossRef] [PubMed]
94. Choi, H.; Larsen, B.; Lin, Z.-Y.; Breitkreutz, A.; Mellacheruvu, D.; Fermin, D.; Qin, Z.S.; Tyers, M.; Gingras, A.-C.; Nesvizhskii, A.I. SAINT: Probabilistic scoring of affinity purification-mass spectrometry data. *Nat. Methods* **2011**, *8*, 70–73. [CrossRef] [PubMed]
95. Sowa, M.E.; Bennett, E.J.; Gygi, S.P.; Harper, J.W. Defining the human deubiquitinating enzyme interaction landscape. *Cell* **2009**, *138*, 389–403. [CrossRef] [PubMed]
96. Mellacheruvu, D.; Wright, Z.; Couzens, A.L.; Lambert, J.-P.; St-Denis, N.A.; Li, T.; Miteva, Y.V.; Hauri, S.; Sardiu, M.E.; Low, T.Y.; et al. The CRAPome: A contaminant repository for affinity purification-mass spectrometry data. *Nat. Methods* **2013**, *10*, 730–736. [CrossRef] [PubMed]
97. Rogers, H.T.; Gregorich, Z.R.; Gant, M.S.; Gao, Z.; Chamot-Rooke, J.; Ge, Y. Proteoforms in disease: Biomedical applications of top-down proteomics. *Mass Spectrom. Rev.* **2026**. [CrossRef] [PubMed]
98. Smith, L.M.; Kelleher, N.L.; Consortium for Top Down Proteomics. Proteoform: A single term describing protein complexity. *Nat. Methods* **2013**, *10*, 186–187. [CrossRef] [PubMed]
99. Schlüter, H.; Apweiler, R.; Holzhütter, H.-G.; Jungblut, P.R. Finding one's way in proteomics: A protein species nomenclature. *Chem. Cent. J.* **2009**, *3*, 11. [CrossRef] [PubMed]
100. Aebersold, R.; Agar, J.N.; Amster, I.J.; Baker, M.S.; Bertozzi, C.R.; Boja, E.S.; Costello, C.E.; Cravatt, B.F.; Fenselau, C.; Garcia, B.A.; et al. How many human proteoforms are there? *Nat. Chem. Biol.* **2018**, *14*, 206–214. [CrossRef] [PubMed]
101. Fröhlich, K.; Fahrner, M.; Brombacher, E.; Seredynska, A.; Maldacker, M.; Kreutz, C.; Schmidt, A.; Schilling, O. Data-independent acquisition: A milestone and prospect in clinical mass spectrometry-based proteomics. *Mol. Cell. Proteom.* **2024**, *23*, 100800. [CrossRef] [PubMed]
102. Perez-Riverol, Y.; Bandla, C.; Kundu, D.J.; Kamatchinathan, S.; Bai, J.; Hewapathirana, S.; John, N.S.; Prakash, A.; Walzer, M.; Wang, S.; et al. The PRIDE database at 20 years: 2025 update. *Nucleic Acids Res.* **2025**, *53*, D543–D553. [CrossRef] [PubMed]
103. Fazal, F.M.; Han, S.; Parker, K.R.; Kaewsapsak, P.; Xu, J.; Boettiger, A.N.; Chang, H.Y.; Ting, A.Y. Atlas of subcellular RNA localization revealed by APEX-seq. *Cell* **2019**, *178*, 473–490.e26. [CrossRef] [PubMed]
104. Berthias, F.; Bilgin, N.; Smyrnakis, A.; Le Boiteux, E.; Kosmopoulou, M.; Albers, C.; Suckau, D.; Mecinović, J.; Papanastasiou, D.; Jensen, O.N. Top-down sequencing of intact proteoforms using the timsOmni mass spectrometer: Accurate determination of co-occurring histone modifications. *Mol. Cell. Proteom.* **2026**, *25*, 101640. [CrossRef] [PubMed]
105. Hirsch, J.D.; Eslamizar, L.; Filanoski, B.J.; Malekzadeh, N.; Haugland, R.P.; Beechem, J.M.; Haugland, R.P. Easily reversible desthiobiotin binding to streptavidin, avidin, and other biotin-binding proteins: Uses for protein labeling, detection, and isolation. *Anal. Biochem.* **2002**, *308*, 343–357. [CrossRef] [PubMed]
106. Guillemette, S.; Serra, R.W.; Peng, M.; Hayes, J.A.; Konstantinopoulos, P.A.; Green, M.R.; Cantor, S.B. Resistance to therapy in BRCA2 mutant cells due to loss of the nucleosome remodeling factor CHD4. *Genes Dev.* **2015**, *29*, 489–494. [CrossRef] [PubMed]

107. Wang, W.; Cai, C.; Qin, S.; He, L.; Liang, Q.; Tang, S.; Xie, J.; Long, T.; Hou, J.; Kim, W.; et al. PARP inhibitors and breast cancer: From therapeutic breakthrough to resistance challenge. *Exp. Mol. Med.* **2026**, *58*, 981–992. [CrossRef] [PubMed]
108. Ray Chaudhuri, A.; Callen, E.; Ding, X.; Gogola, E.; Duarte, A.A.; Lee, J.E.; Wong, N.; Lafarga, V.; Calvo, J.A.; Panzarino, N.J.; et al. Replication fork stability confers chemoresistance in BRCA-deficient cells. *Nature* **2016**, *535*, 382–387, Erratum in *Nature* **2016**, *539*, 456. [CrossRef] [PubMed]

Disclaimer/Publisher's Note: The statements, opinions and data contained in all publications are solely those of the individual author(s) and contributor(s) and not of MDPI and/or the editor(s). MDPI and/or the editor(s) disclaim responsibility for any injury to people or property resulting from any ideas, methods, instructions or products referred to in the content.